Process simulation and techno-economic assessment of Salicornia sp. based jet fuel refinery through Hermetia illucens sugars-to-lipids conversion and HEFA route

Fredsgaard, Malthe; Hulkko, Laura Sini Sofia; Chaturvedi, Tanmay; Thomsen, Mette Hedegaard

Published in:
Biomass & Bioenergy

DOI (link to publication from Publisher):
10.1016/j.biombioe.2021.106142

Publication date:
2021

Document Version
Publisher's PDF, also known as Version of record

Biomass and Bioenergy 150 (2021) 106142

Contents lists available at ScienceDirect

Biomass and Bioenergy

journal homepage: www.elsevier.com/locate/biombioe

Research paper

Process simulation and techno-economic assessment of *Salicornia* sp. based jet fuel refinery through *Hermetia illucens* sugars-to-lipids conversion and HEFA route

Malthe Fredsgaard *, Laura Sini Sofia Hulkko, Tanmay Chaturvedi, Mette Hedegaard Thomsen

Department of Energy Technology; Aalborg University, Niels Bohrs Vej 8, 6700 Esbjerg, Denmark

ARTICLE INFO

Keywords:
Halophyte
Salicornia sp.
HEFA-SPK
Hermetia illucens
SuperPro Designer

ABSTRACT

Succulent halophyte *Salicornia* sp. was characterized to evaluate its suitability for biorefinery, as soil salinization is seen as a major agricultural issue and the demand for biofuel is increasing. Green fractionation of biomass approach was chosen, with liquid and solid fractions of the biomass considered separately. Soxhlet extractions were used to separate different biochemical groups from the pulp, and the lignocellulosic residue was hydrothermally pretreated, enzymatically hydrolyzed, mixed with an existing agricultural feedstock, and fed to black soldier fly larvae (BSFL) for sugars-to-lipids conversion. The ASTM approved route of hydroprocessed esters and fatty acids (HEFA) was applied using *in silico* study of processing BSFL lipids to sustainable jet fuel, using SuperPro Designer and Aspen HYSYS. Simulations and techno-economic assessment showed, with the applied process routes, inputs and production rates, the biorefinery process will be profitable in 7 years, with a biomass input flow rate of over 60 ton h^{-1} *Salicornia* sp. with decreasing payback time as the biomass input flow rate increases. Therefore, *Salicornia* sp. feedstock and sugars-to-lipids conversion method for biorefinery and liquid fuel production can function as a feasible biorefinery process with a normalized CO_2-e reduction of HEFA-SPK of 95.5% compared to similar fossil fuels.

1. Introduction

An increase in public climate awareness has pushed the European Union (EU) to set aviation sustainability goals for 2050 with a 75% reduction in CO_2 emissions per passenger kilometer, a 90% reduction in total NO_x emissions, and a 65% noise reduction compared to a typical new aircraft of the year 2000 [1]. These emission reduction goals are ambitious, as the yearly passenger-kilometers will rapidly increase the aviation carbon footprint, if conventional fossil fuels are being used [2]. To reach the said goals, the production capacity of sustainable jet fuels has to be increased all over the world, as the share of sustainable aviation fuel in 2019 in the fuel aviation fuel blend was 0.05 w%, and increasing this share above 2 w% requires research in new conversion methods apart from what has already been researched [3]. Biofuels can be made from excess 2nd generation biomass, which would otherwise be considered biowaste, hence not compete with food production. To make use of this excess biomass, it has to be processed into a usable biorefinery feedstock and preferably not compete with human food production, e.g. vegetable oil production. Bann et al. in 2016 compared the financial potential for different biofuel refinery processes, and found Hydroprocessed Esters and Fatty Acids-Synthetic Paraffinic Kerosene (HEFA-SPK) to be the cheapest bio-jet fuel to produce, even when changing the lipid feedstock input of the biorefinery simulation [4]. Multiple lipid feedstocks are available for oil to jet fuel conversion, as oils and paraffins are similar in molecular structure to alkanes in the jet fuel range. As jet fuel comprises of alkanes in the range of 8 to 16 carbon atoms per molecule, free fatty acids (FFA) from depropanation of oils, and paraffins with slightly higher molecule lengths, are ideal feedstocks for HEFA-SPK production [5]. Fuel properties of jet fuel, such as freezing point temperature, kinematic viscosity, and density, are strictly specified by ASTM to ensure high quality and a dependable fuel, which again is determined by refining conditions. A difference in refining conditions will show differences in alkane length, isomerization, carbon-to-hydrogen ratio, and thereby fuel properties. Especially isomerization of n-alkanes in the HEFA-SPK process route is crucial, as isomerization will lower the freezing point temperature, and alter other thermodynamical properties to resemble the commonly used jet fuel, Jet A-1 [6].

Living organisms have developed digestion systems suitable for various kinds of substrates, and in recent years, the interest of using insect digestion for lignocellulosic biomass conversion has increased [7].

* Corresponding author.
E-mail address: mfre@et.aau.dk (M. Fredsgaard).

https://doi.org/10.1016/j.biombioe.2021.106142
Received 4 January 2021; Received in revised form 19 May 2021; Accepted 23 May 2021
Available online 31 May 2021

Hermetia illucens, commonly known as black soldier fly larva (BSFL), can be used as a novel bio-waste treatment to convert organic waste, such as manure, fruit, or vegetable waste, into high protein and high lipid animal feed [8,9]. Trends show insect-based animal feeds can be produced in a more sustainable way than conventional feed crops, partly because of the large array of feeds the BSFL can digest [10]. Using BSFL is an easy, cheap, and scalable bio-waste treatment from biomass to lipids and valuable compounds, such as protein, organic fertilizer, and chitin [10]. The annual halophyte *Salicornia* sp. is used worldwide as a gourmet vegetable, but after the growing period, the biomass lignifies, and cannot be used for food production. This residual biomass has great potential for phytochemical extractions, as the plant contains large amounts of antioxidants with great medicinal properties [9,11–14]. Approximately 17,300 kg ha^{-1} yr^{-1} lignified *Salicornia persica* has been reported to be left over after cultivation at optimal conditions, and shows to be a large problem for the halophyte farmers, as the biomass contains high concentrations of salts, making incineration or composting impractical. Furthermore the cultivation of *Salicornia* sp. can happen on salt affected lands, and due to its bioremediation properties, it will be capable of decreasing salt content in soil [15,16]. In this study, *Salicornia* sp. found in the Wadden Sea area of northern Europe, will be fractionated and processed into value-added streams and a lignocellulosic waste product. This waste product will be converted into lipids and high-value co-products, and further refined into biofuels. Thus, the idea of circular economy will be implemented to use all possible components of the feedstock, and seen as a route for sustainable and feasible production of 2nd generation biomass to fuel.

2. Materials and methods

Biomass characterization experiments, mass balances and a simulation from biomass to HEFA-SPK and value-added components, as shown by process overview in Fig. 1, were made to determine the biofuel yield and feasibility by a techno-economic assessment (TEA) using Intelligen SuperPro Designer (SPD). *Salicornia* sp. was simulated as a biorefinery feedstock, extracted crude high-value secondary metabolites, and excess lignocellulosic biomass underwent hydrothermal pretreatment to break the lignocellulosic structure for cellulase to hydrolyze the cellulose into glucose. This pretreated slurry was simulated to be fermented for BSFL to digest using a lactic acid-producing bacteria culture, and BSFL was fractionated into fractions of lipids, protein, a solid residue containing chitin, and aqueous waste products. The BSFL lipids were hydrogenated, hydrocracked and isomerized. Fuels in the molecular range of gasoline, Jet A-1 and diesel, hereon referred to as naphtha, HEFA-SPK, hydrogenated vegetable oil (HVO) respectively, and alkane flash products were produced.

Experimental work for modeling inputs

2.1. Salicornia sp. biomass characterization

Data inputs for the *Salicornia* sp. biorefining simulation were all obtained through laboratory scale experiments, done on the biomass sampled 11th November 2019. For the biochemical characterization of the primary metabolites of *Salicornia* sp., the halophytic biomass was sampled from the Danish Wadden sea national park, coordinates: 55.307733,8.652292, on 15th October 2019 and 11th November 2019. Characterization of the primary metabolites was done on the biomass sampled 15th October 2019, and BSFL feed trials were done using the biomass sampled 11th November. The biomass was rinsed using tap water, fractionated into a solid (pulp) and liquid (juice) fraction using a domestic single horizontal auger screw press (Omega EUJ-707, Sana, Czech Republic). The pulp was dried in a 50 °C forced ventilation oven and milled using a knife mill (GM200, Retsch, Germany) at 10,000 rpm for 45 s. Suitable lactic acid-producing bacteria, with high survival and reproductive rate in saline conditions, were chosen to be simultaneously added to the juice, for an *in situ* lactic acid-producing bacteria cultivation.

Laboratory scale extractions of lipids, secondary metabolites, salts, and other organic material were performed using the Soxhlet extraction method [17]. Lipids were extracted using n-hexane, and a sequential extraction using ethanol (EtOH) extracted secondary metabolites, salts, and other organic compounds. Salt removal by Soxhlet EtOH extraction was verified post extractions using a protocol developed by the National Renewable Energy Laboratory (NREL) for ashing, which showed a 100 w% removal of ashes [18]. Extractions were performed using 7–10 g dried and milled *Salicornia* sp. to 150 ml solvent, and weighed before, between, and after each extraction to determine the mass of the extracts. The weighing was performed after solvent evaporation and drying of the biomass and Soxhlet thimbles. The extracted lipids from *Salicornia* sp. are expected to have a high nutritional value, as similar species of *Salicornia* spp. show to have content of healthy polyunsaturated fatty acids [19,20]. Total nitrogen was determined with modified Dumas combustion method, and crude protein was approximated with a 6.0 conversion factor, as a higher conversion factor of 6.25 tend to overestimate the protein content [21,22]. Sugars and lignin in lignocellulose were determined by strong acid hydrolysis followed by ashing of the remaining non-acid soluble material and high-performance liquid chromatography (HPLC) analysis. For further details on characterization done on *Salicornia* sp. before SPD simulation, the authors refer to the work done by Hulkko and Fredsgaard (manuscript in preparation).

2.2. Hermetia illucens characterization

In cooperation with Enorm Biofactory A/S feed trials on BSFL have been made. The trials were 100 w% chicken feed (CF) and 60/40 w% CF and extractive free *Salicornia* sp. respectively. The feedstocks had a dry matter (DM) content of 30 w% with a feed mass of 1150 g. After a growing period of 14 days, the larvae were separated from the remaining feed and frass and devitalized using steam. The larvae were dried using a 50 °C forced ventilation oven for 48 h. The lipid content of the BSFL was determined by the Soxhlet extraction method using n-hexane [17]. Large scale data regarding phase separation of the solid and liquid phase of the BSFL by 50 °C heated screw press, protein content, and water content were given by Enorm Biofactory A/S [23]. Feed trials using pretreated and hydrolyzed extractive free *Salicornia* sp. have not been made, and BSFL composition data for simulation is based on intermediate characterization values of 100 w% CF and 60/40 w% CF and extractive-free *Salicornia* sp. respectively.

Modeling methods

Each subsection will refer to one or more numbers on Fig. 1 for a better process overview.

2.3. Salicornia sp. biorefining simulation (1–4)

The *Salicornia* sp. biorefining simulation is split up into four overall steps: preprocessing, n-hexane Soxhlet extraction, EtOH Soxhlet extraction, and pretreatment/enzymatic hydrolysis.

Preprocessing of the biomass consisted of an initial green fractionation into pulp and juice by screw pressing. After screw pressing, the remaining water was evaporated off, and the dried biomass was shredded.

After shredding, the biomass was transported to the first of two Soxhlet extractions. As SPD does not have a Soxhlet extraction unit, the extraction was modeled using relevant sub-components. The modeled Soxhlet cycle was simulated as a semi-continuous reaction, as the new solvent continuously entered the extractor unit, but the solids were

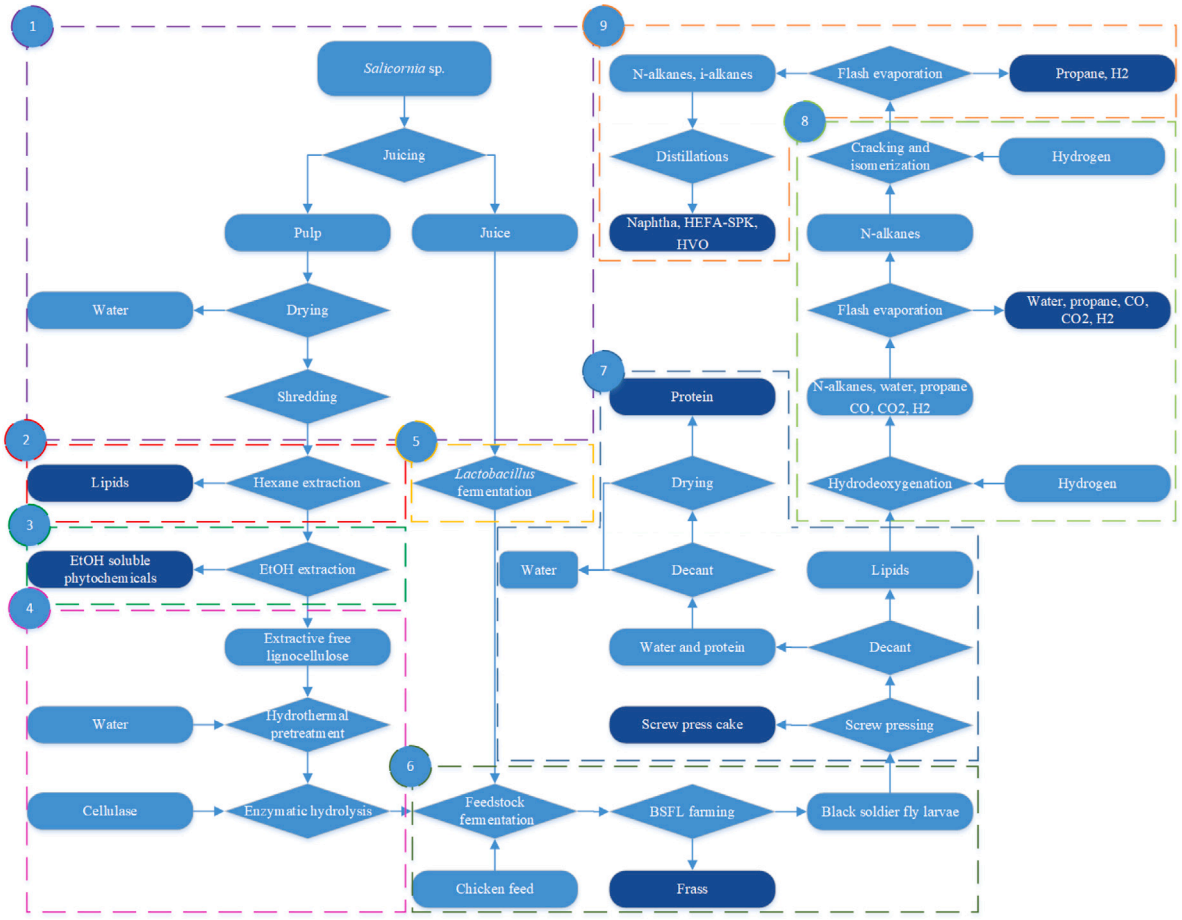

Fig. 1. Full schematic overview of the process presented in this paper. Diamond figures are process equipment or sub-processes, rectangular figures are material, dark blue rectangles are products and co-products. SuperPro Designer simulation layout can be seen in Figs. 7 to 15. Section 1: Preprocessing of *Salicornia* sp. Section 2: N-hexane Soxhlet extraction. Section 3: Ethanol Soxhlet extraction. Section 4: Hydrothermal pretreatment and enzymatic hydrolysis of extractive free lignocellulosic *Salicornia* sp. Section 5: *Lactiplantibacillus plantarum* cultivation in *Salicornia* sp. juice. Section 6: BSFL feedstock fermentation and BSFL cultivation. Section 7: BSFL processing. Section 8: BSFL lipid hydrodeoxygenation and hydrocracking and isomerization. Section 9: Fuel distillation. (For interpretation of the references to color in this figure legend, the reader is referred to the web version of this article.)

suspended in the extraction unit with a retention time of 1 h for n-hexane extraction and 6 h for EtOH extraction. The cycle consisted of a continuous storage unit (Soxhlet extraction chamber), evaporation unit, using low-pressure mechanical vapor recompression (Soxhlet siphon), custom mixing make-up valve (continuously added solvent), and solvent buffer tank (round bottom flask). The low-pressure stream was recondensed by compression after the evaporation unit to ensure a liquid phase, hence there would be no phase change inside the rotational machinery that would cause equipment damage. The evaporator unit would recycle 99 w% of the solvent, which was the default value provided by SPD. 99 w% of the remaining solvent and solvent solubles got decanted off and stored in a storage unit. To provide a pure concentrate of the extracted compounds, the solvents would get fully vented off in the storage unit, and recycled back into the Soxhlet extraction cycle. The overall recycling of the solvent is therefore 99.99 w%, and the remaining solvent would evaporate off during biomass transportation.

The extractive free biomass, consisting of lignocellulose and denatured protein, was simulated to be pretreated as described by Alassali et al. on *S. sinus-persica* [24]. The optimal hydrothermal pretreatment conditions, followed by fermentation, for highest EtOH yield was shown to be 170 °C for 10 min with a conversion of 76.9%. As the biomass was used as feedstock, the chosen hydrolysis method was enzymatic hydrolysis, as strong acid hydrolysis would affect the quality of the feedstock for insect consumption. Using data from literature [24–28] and the value for cellulose of 24.5 g/100 gDM obtained from previous characterization work done by the authors, the amount of cellulase added to the hydrothermally pretreated slurry was calculated as described in Eq. (1), where $\dot{m}_{cellulase}$ is the mean mass flow rate of cellulase provided to the batch enzymatic hydrolysis reactor, $\dot{m}_{cellulose}$ is the mean mass flow rate of cellulose of the slurry provided to the batch enzymatic hydrolysis reactor, $FPU_{loading}$ is the filter paper activity per unit mass of lignocellulosic DM, FPU_{batch} is the filter paper activity of the batch of enzymes per mL, $\rho_{cellulase}$ is the density of cellulase and 76.9 % is the conversion from the paper of Alassali et al. [24].

Table 1
Enzyme calculation data.

Parameter	Symbol	Value	Unit
Mass flow, cellulose	$\dot{m}_{cellulose}$	100	kg h^{-1}
Activity	$FPU_{loading}$	15	FPU g^{-1}
Activity	FPU_{batch}	75	FPU mL^{-1}
Density	$\rho_{cellulase}$	1.2	g mL^{-1}
Mass flow, enzyme	$\dot{m}_{cellulase}$	31.2	kg h^{-1}

$$\dot{m}_{cellulase} = \frac{\dot{m}_{cellulose} \cdot FPU_{loading} \cdot \rho_{cellulase}}{FPU_{batch} \cdot 76.9\ \%} \quad (1)$$

The high mass ratio of cellulase to cellulose is based on laboratory scale enzymatic hydrolysis for optimal performance, and is considered to be very high for full-scale production. It should also be noted that the cellulase is suspended in a liquid, and is therefore a suspension and not a pure enzyme mixture, hence the high enzyme concentration [28] (see Table 1).

2.4. Hermetia illucens biorefining simulation (5–7)

As BSFL are hatched from fly eggs, an initial larvae culture needs to be made. Enorm Biofactory A/S is doing this in simple fly-cages, where the flies lay eggs in-between pieces of cardboard. This was simulated to happen continuously in a drum, with a small portion of the produced prepupae larvae as input and fly eggs as output. Black soldier flies do not need food as they are mating, but only an insignificant amount of water [23]. In SPD, the cultivation of BSFL was simulated as a silo with specific conditions and the residence time of 14 days. In reality, the cultivation is happening in separate parallel rooms with suitable ambient conditions, and the larvae are laying in trays placed in racks to make the transferring easier.

After the cultivation of BSFL, the larvae and frass were simulated separated by a coarse screen. The frass was simulated stored in a big silo. A small amount, 1 w% of the total amount of cultivated BSFL, was transferred into the drum to allow for pupation and lay eggs to maintain the number of input larvae. The remaining BSFL were devitalized using steam and transported to a storage unit. The storage unit was needed as the cultivation of BSFL was batch cultivation, and intermediate storage would allow for a continuous output flow rate. From the storage unit, the BSFL were pressed using a hot screw press. Given by data from Enorm Biofactory A/S, the screw press separates the liquid phase containing lipids, water, and protein from the solid phase containing the BSFL exoskeleton and residual matter from the BSFL. The exoskeleton was high in chitin and could be sold as a value-added product. After screw pressing, the lipid and water phases were separated. Solid protein was separated from the water, dried, and sold as a value-added product.

2.4.1. In situ lactic acid-producing bacteria production

Feeding of BSFL typically lasts 14 days, hence the feedstock was required to stay fresh for a period of 14 days and the growth of mold should be inhibited. To ensure a feedstock of high quality, a culture of lactic acid-producing bacteria was added to the feedstock to allow for lactic acid fermentation. *In situ* production of lactic acid-producing bacteria using *Salicornia* sp. juice was desired, as this would lower the operation cost of the biorefinery, and utilize a waste stream. Small scale feedstock trials done by Enorm Biofactory A/S used the Danish commercial dairy product A38 by Arla, containing *Lactobacillus acidophilus* in a ratio of 1:22 dairy product to feedstock. As *Lactobacillus acidophilus*, used by Enorm Biofactory A/S, was salt-tolerant up to 5 g L^{-1} NaCl, the juice fraction from the initial screw pressing could not be used as a culture medium for the *in situ* production of *Lactobacillus acidophilus* [29]. The ashing results of *Salicornia* sp. juice showed the juice contained an ash content of 11 g L^{-1}, with the majority of the ash from the juice expected to be salt, as shown by the authors Hulkko and Fredsgaard (manuscript in preparation). *Lactiplantibacillus plantarum* (LBP), previously defined by the taxonomy *Lactobacillus plantarum*, known for its high salt tolerance, was chosen to be simulated for *in situ* lactic acid production. LBP has shown optimal growth up to 60 g L^{-1} NaCl and to be able to grow at pH 4–8 [30]. This made LBP an ideal candidate for *in situ* production of lactic acid-producing bacteria, to be used in feedstock fermentation.

2.5. HEFA-SPK process simulation (8)

The HEFA-SPK process route is a process with the input of lipids and hydrogen and output of n-alkanes, i-alkanes, propane, water and CO and CO_2. This process was simulated in two reactors: hydrodeoxygenation (HDO) reactor and hydrocracking and isomerization (HI) reactor. In each reactor, multiple parallel reactions occurred. In the HDO packed bed reactor (PBR), the BSFL lipid underwent the following reactions: hydrogenation of triglycerides, depropanation, decarboxylation (DCO_2), decarbonylation (DCO), synthesis of intermediate aldehyde and alcohol products, and HDO of alcohol to n-alkane [6]. The lighter gaseous products were separated by flash separation, and the liquid n-alkanes were further processed in a HI reactor. The mixture of alkanes could then be distilled to yield naphtha, HEFA-SPK, and HVO with specified predetermined distillation temperatures.

2.5.1. Hydrogenation of triglycerides

In the HEFA process route, the lipid feedstock often consists of a mixture of saturated, mono-unsaturated, and poly-unsaturated triglycerides. HEFA-processing unsaturated triglycerides would result in the formation of alkenes, with less desirable combustion characteristics, therefore the initial hydrogenation of unsaturated triglycerides was crucial. As the triglyceride profile of terrestrial animals is often higher in saturated triglycerides than oil-producing crops, the saturation of the unsaturated fatty acids from animal fat is less hydrogen intensive [31]. An example of saturation of cis-unsaturated triglyceride is the saturation of monounsaturated triglyceride triolein (tri-C18:1) into the saturated triglyceride, tristrearin (tri-C18:0). This process can be done at a temperature of 175 °C and a pressure of 0.55 MPa with nickel as a catalyst [32].

Reaction 1:

$$C_nH_{(2n-1-6m)}(COOH)_3 + ({}_3m)H_2 \xrightarrow{Ni} C_nH_{(2n-1)}(COOH)_3$$

where n is the number of carbon atoms in the triglyceride aliphatic chain, m is the number of double bonds in each aliphatic chain. The conversion factor for saturation of tri-C18:1 can be found by the research of Swicklik et al. and a reaction rate constant can be calculated [32]. As the difference in molecular structure between long-chain triglycerides is not considered to be big, all unsaturated triglycerides are simulated to react at the same rate.

2.5.2. Depropanation

Triglycerides comprise of a glycerin backbone and three fatty acid branches. These can be separated by a catalytic reaction using hydrogen as reactant, yielding propane and FFAs [33]. In the reaction equation of the depropanation of saturated triglycerides, n is the number of carbon molecules in the FFAs. The used catalyst, nickel with molybdenum promoted aluminum oxide (Ni-Mo/Al_2O_3), is described by Sinha et al. in the review of HEFA processing [33].

Reaction 2:

$$C_nH_{(2n-1)}(COOH)_3 + 3\ H_2 \xrightarrow{Ni-Mo/Al_2O_3} 3\ C_nH_{2n+1}COOH + C_3H_8$$

2.5.3. Hydrodeoxygenation

To produce n-alkanes from the saturated FFAs, the carboxyl groups of FFA molecules needed to be removed and replaced with hydrogen, or the oxygen removed in a HDO reactor. HDO is not a straight reaction route, as some reaction intermediates will be produced. In a study by Arora et al. [34] investigating the synthesis of octadecane (C18) from the FFA stearic acid (C18:0) using the catalyst Ni-Mo/Al_2O_3, reaction intermediates octadecanal (C18=0) and octadecanol (C18-OH) were found, with heptadecane (C17) being a by-product from direct DCO_2

of C18:0 and decarbonylation of C18=O. These aldehyde and alcohol reaction intermediates, will further react with hydrogen to form C18, as shown in Fig. 2. Martinez-Hernandez et al. determined by simulation in SPD the ratios of HDO, DCO_2 and DCO to be 60.1 w%, 36.1 w% and 3.8 w% respectively for palm oil [6]. Reaction 3–7 can be seen in Fig. 2.

Reaction 3: $C_{18:0} + H_2 \xrightarrow{Ni-Mo/Al_2O_3} C_{18} = O + H_2O$

Reaction 4: $C_{18:0} \xrightarrow{Ni-Mo/Al_2O_3} C_{17} + CO_2$

Reaction 5: $C_{18} = O + H_2 \xrightarrow{Ni-Mo/Al_2O_3} C_{17} + CO$

Reaction 6: $C_{18} = O + H_2 \xrightarrow{Ni-Mo/Al_2O_3} C_{18} - OH$

Reaction 7: $C_{18} - OH + H_2 \xrightarrow{Ni-Mo/Al_2O_3} C_{18} + H_2O$

2.6. Hydrocracking and isomerization (8)

To make the fuel products meet the ASTM standards set for HEFA-SPK, the n-alkanes were hydrocracked and isomerized. This would result in a lower freezing point of the fuel while maintaining high energy released from combustion. The two reaction types, hydrocracking, and isomerization would happen simultaneously in a PBR, with the presence of free excess hydrogen. Hydrocracking is the reaction where long-chained alkanes are split into two smaller alkanes and saturated with hydrogen to prevent the formation of alkenes. Isomerization is the reaction of rearranging the atoms in alkanes, for example, from n-decane to i-decane. Successful research has been done considering HI of vegetable oils and non-edible oils and fats [35–39], but HI is typically performed to fossil crude hydrocarbons, to satisfy the demand for lighter hydrocarbon fractions [6].

Studies of HI on n-alkanes in the range of C8–C18 were done by Flinn et al. [40] and Coonradt et al. [41], and backed up by Martinez-Hernandez et al. [6], giving a set of possible reactions of HI, reaction 8–12. It should be noted, the number of carbon atoms in the molecules of biofuel is similar to the number of carbon atoms, and general structure, in the FFA chains of BSFL lipids [31]. All hydrocracking reactions were splitting alkanes into the range C8–C15, which has molecules within the jet fuel range. This will happen simultaneously with isomerization.

Hydrocracking

Reaction 8:

$C_nH_{2n+2} + H_2 \longrightarrow C_{n-3}H_{2n-4} + C_3H_8$ for n = 13 – 18

Reaction 9:

$C_nH_{2n+2} + H_2 \longrightarrow C_{n-8}H_{2n-14} + C_8H_{18}$ for n = 17 – 18

Reaction 10:

$C_nH_{2n+2} + H_2 \longrightarrow C_{n-7}H_{2n-12} + C_7H_{16}$ for n = 17 – 18

Reaction 11:

$C_nH_{2n+2} + H_2 \longrightarrow 2\ C_{n/2}H_{n+2}$ for n = 16, 18

Isomerization

Reaction 12:

$C_nH_{2n+2} \longrightarrow iso - C_nH_{2n+2}$ for n = 6 – 18

Reactions 8–11 occur simultaneously for C16–C18, followed by reaction 8 for C13–C15, and finally all isomerization reactions occur. As reactions 8–11 occurs simultaneously for C18, only 16.1 w% of the initial C18 is left. Of that, isomerization occurs for 18.9 w%, leaving 13.1 w% C18 in the final fuel, of the initial amount (see Table 2).

Table 2
HI reactions defined in mass percentage as suggested by Martinez-Hernandez et al. [6].

	Reaction yield [%]				
	Reaction 8	Reaction 9	Reaction 10	Reaction 11	Reaction 12
C3	–	–	–	–	–
C7	–	–	–	–	–
C8	–	–	–	–	90
C9	–	–	–	–	88
C10	–	–	–	–	90
C11	–	–	–	–	90
C12	–	–	–	–	90
C13	5.8	–	–	–	90
C14	61.7	–	–	–	53.9
C15	51.3	–	–	–	27.2
C16	37.1	–	–	18.0	6.0
C17	50.4	17.3	2.0	–	12.6
C18	4.9	41.9	13.9	23.2	18.9

Table 3
Fuel limits for Jet A-1 as reported by Stark et al. [42].

Parameter	Jet A-1	Unit
Density at 15 °C	775–840	kg m^{-3}
Max. sulfur content	0.3	w%
Max. total aromatics	26.5	vol%
Max. T10	205	°C
Max. T90–T10	300	°C
Max. final point	>22	°C
Max. freezing point	−47.0	°C
Max. viscosity at −20 °C	8.0	$mm^2\ s^{-1}$
Flash point	38.0	°C

2.7. Distillation (9)

Distillation was simulated using the Aspen HYSYS process design tool, as SPD does not calculate complex azeotropic thermodynamic properties of alkanes, which were necessary to know to comply with ASTM standards shown in Table 3. Distillation took place in two separate columns, where the first column separates the HI alkanes in the gasoline range, and the second column separates the jet fuel range from the diesel range.

After HI of the fuel, some gaseous C_3H_8, H_2O, H_2, CO, CO_2 and other light alkanes, due to the azeotropic properties of the alkane mixture, would be flashed off to ensure a purer crude fuel. If these molecules were not flashed off, it would greatly affect the properties of especially the distilled naphtha, and water would complicate distillation.

For naphtha distillation, the heavy key simulation distillation temperature, where the distilled molecule with the highest boiling point would boil, was 190 °C, which was the mean value of 175 °C and 205 °C, as proposed by Leffler et al. [43]. This temperature was also considered to be a reasonable light key distillation temperature of HEFA-SPK, where the distilled molecule with the lowest boiling point will boil, of HEFA-SPK [42]. The heavy key temperature of 220 °C is chosen, as Jet A-1 fuel range molecules, can be distilled in the temperatures of 175–315 °C, but temperatures of 175–205 °C and 300–315 °C could yield unwanted physical properties for the jet fuel product [42]. The freezing point of HEFA-SPK was set as one of the primary constraints in the distillation simulation in Aspen HYSYS. As the freezing point was not determined directly in Aspen HYSYS, it is calculated using Eq. (2) based on the data of freezing points of n-alkanes, estimated freezing points of i-alkanes from Martinez-Hernandez et al. [6], and the molar fractions of alkanes of the distilled jet fuel stream (see Fig. 3).

$$FP_{Jet\ A-1} = \sum_{i=C8}^{C18} FP_i y_i \quad (2)$$

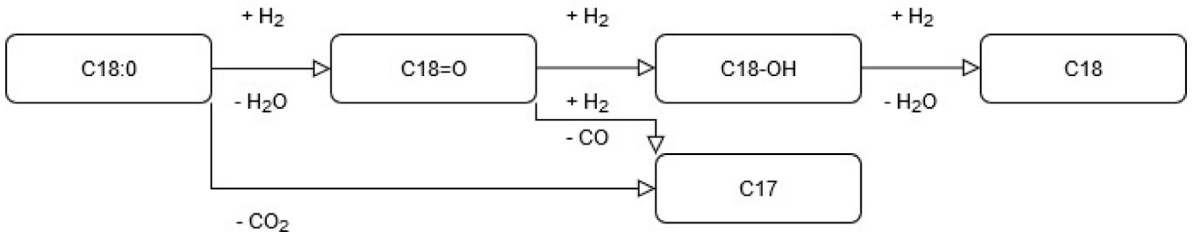

Fig. 2. Possible reactions HDO, DCO_2 and DCO reactions for C18:0.

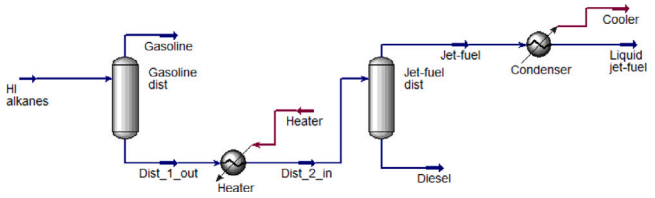

Fig. 3. Schematic of distillation from Apsen HYSYS.

2.8. Techno-economic assessment

A techno-economic assessment (TEA) is a crucial step when planning the construction of a processing plant or inputting new process units and material streams to existing process plants. To analyze the costs and revenues correlated to the production of sustainable jet fuel, the SPD tool allows the user to examine the Economic Evaluation Report (EER) showing detailed information about costs and revenues from each production stream. Capital expenditure (CAPEX) and operational expenditure (OPEX) are functions of the process plant size, and corresponding building costs, staff salaries, material and chemical costs, and utility used for heating and cooling.

Labor rates were assigned for all processing units and for simplification, all equipment types have the same type of labor assigned. In SPD, the labor cost (LC) was determined from the basic salary, x, and the model was run using the mean salary of operators in Denmark being 20.6 USD h^{-1} [44]. On top of that, SPD took other labor-related costs in the form of coefficients and required labor hours, h, into account.

$$LC = x_i \cdot (1 + a + b + o + s) \cdot h \quad (3)$$

where a is administrative costs (0.6), b is benefits (0.4), o is operating supplies (0.1) and s is supervision (0.2), which were default coefficients from SPD.

Energy required for heating and cooling of streams under 140 °C was provided by utility such as steam at 152 °C and cooling water at 25–30 °C, with a heat transfer coefficient of 1500 W m^{-2} $°C^{-1}$ and efficiency of 100%. All tanks and fermentors with the capability of stirring had stirring at 200 W m^{-3}. Most pumps in the simulated process were inputted to overcome pipe pressure losses, with the pressure difference being between 1 bar and 0.1 bar.

2.9. Simulation parameters

For easy manipulation of input flows for sensitivity analysis, all input streams were controlled from one master input. This master input stream was split into its respective components of *Salicornia* sp., water for pretreatment, cellulase, CF, and hydrogen. All figures showing SPD schematics have a red dot for the main input and a blue dot for the main output, see Figs. 7–15. To ease building the process, the user can utilize the unit procedure *Continuous* 1 × 1 *reaction generic box*, see Fig. 12.

Table 4
Operation and simulation parameters 1. All parameters determined by laboratory work.

Parameter	Value	Unit
Preprocessing of *Salicornia* sp. (Fig. 7)		
Screw press separation efficiency	100	%
Drum drying efficiency	100	%
Soxhlet extractions (Figs. 8 & 9)		
Solvent evaporation	99	w%
Make-up solvent (of extractor volume)	1	w% h^{-1}
Hexane extractor retention time	2	h
Hexane mixing	9.825	g_{hex} $g^{-1}_{biomass}$
Hexane extractives	66.4	$g_{ext.}$ $kg^{-1}_{biomass}$
EtOH extractor retention time	6	h
EtOH mixing	11.835	g_{EtOH} $g^{-1}_{biomass}$
EtOH extractives	35.5	$g_{ext.}$ $kg^{-1}_{biomass}$
Decanter liquid separation efficiency	99	w%

Generic boxes were used in the simulation with meta-data attached if a generic box was imitating a processing unit. Generic boxes can be used for simplifications for the SPD user, as it allows for lower computational time and more flexibility. This unit procedure allows the user to make a pseudo-reaction that does not affect the techno-economic assessment, nor the energy and mass balances. This allowed the formation of non-existing intermediate products. An example of this generic box unit is in Fig. 14, to split the BSFL lipids into its triglyceride profile, as specified in Table 6.

Figs. 7 to 15 show the process built in detail, and with the simulation parameters defined in Tables 4 to 8 lies the foundation for the process simulation. All heating and cooling units were placed separately from reactors, evaporators, distillation towers, etc. as this allowed for inter-stream energy recovery heat exchangers by the built-in process option of energy recovery in SPD, and thereby saving utility expenses.

Table 4 shows the operation and simulation parameters for the *Salicornia* sp. preprocessing, and extractions. The first unit on Table 4, component splitting, is a redundant unit, as the purpose of this unit is to increase flexibility when changing one input stream, so the rest of the streams will scale accordingly. The streams leaving this component splitting unit are inputs for pretreatment, enzymatic hydrolysis, feedstock production and HEFA-SPK processing. Input and output mass flow rates are determined by laboratory-scale experiments. Shedding as a process unit is implemented with the default SPD values.

Table 5 shows the operational parameters for hydrothermal pretreatment, enzymatic hydrolysis, feedstock mixing, stream splitting of *in situ* production of LPB. The stream was split before the *in situ* production unit of LPB was to ensure the right cultivation conditions of LPB. Values regarding hydrothermal pretreatment and enzymatic hydrolysis are based on the work done by Alassali et al. [24].

Table 6 shows the blended hydrolyzed *Salicornia* sp. and CF feedstock operational conditions, feedstock fermentation conditions, BSFL cultivation conditions, BSFL processing conditions and the BSFL lipid profile. Lipid profiles of terrestrial animals are determined by the provided feedstock, thus the lipid profile used in this study, described

Table 5
Operation and simulation parameters 2. All parameters determined by literature and laboratory work [24–30].

Parameter	Value	Unit
Pretreatment and enzymatic hydrolysis (Fig. 10)		
Dry matter (DM) of slurry before pretreatment	6	w%
Pretreatment temperature	140	°C
Pretreatment time	76	min
Hydrolysis temperature	30	°C
Hydrolysis time	24	h
CF:*Salicornia* sp. ratio	60/40	w%
Feedstock DM before sludge drying	14.1	w%
Feedstock DM after sludge drying	30.0	w%
***Lactiplantibacillus plantarum* cultivation** (Fig. 11)		
Component splitting (excess juice:LPB culture ratio)	92.07/7.93	w%
Salicornia sp. storage time	24	h
LPB cultivation temperature	30	°C
LPB fermentation time	24	h
LPB storage time	24	h
Flow splitting (storage:LPB culture ratio)	96.15/3.85	w%

Table 6
Operation and simulation parameters 3. All parameters determined by literature and laboratory work [31].

Parameter	Value	Unit
Feed fermentation and BSFL cultivation (Fig. 12)		
Storage temperature	30	°C
Flow mixing (feedstock:LPB culture ratio)	96.15/3.85	w%
Feedstock fermentation time	24	h
Feedstock storage time	24	h
BSFL cultivation time	14	d
Parallel BSFL cultivation units	14	–
BSFL culture recycle	1	w%
BSFL processing (Fig. 13)		
Devitalization temperature	140	°C
Screw press liquid separation	99	w%
Decanter lipid separation eff.	100	w%
Decanter water separation eff.	70	w%
Drum drying efficiency	100	%
BSFL lipid profile, generic box (Fig. 14)		
Tri-C12:0	39.4	w%
Tri-C14:0	7.6	w%
Tri-C16:0	18.6	w%
Tri-C18:0	5.0	w%
Tri-C18:1	23.6	w%
Tri-C18:2	5.8	w%

by Li et al. [31], might deviate from the actual lipid profile of a BSFL culture partially fed with hydrolyzed *Salicornia* sp. Lipid profile of BSFL from Li et al. was obtained from chicken manure fed BSFL [31].

Table 7 shows a summary of the HEFA process route conditions. As the exit temperature of the HDO is 100 °C, and some of the products of the HDO reaction is water, some water will be in vapor phase and some in liquid phase. The flash evaporation column is cooled to 50 °C in order to get a clear separation between the volatile non-polar n-alkanes and the polar water. As the flow separation of hydrogen is set to 50/50 w%, the relative amount of hydrogen in the HI reactor compared to the HDO reactor, is higher. As a low amount of propane, but high amount of longer alkanes, is desirable in the fuel, the propane rich product from the HI reaction is flashed off at a relatively low temperature, 35 °C, before fuel distillation.

Table 8 shows the buying and selling prices of chemicals, bulk materials and utilities. Initial costs of LPB is not included, as the production

Table 7
Operation and simulation parameters 4.All parameters determined by literature study and SPD simulation [6].

Parameter	Value	Unit
Hydrodeoxygenation and HI (Fig. 14)		
H_2 flow separation	50/50	w%
HDO input temperature	310	°C
HDO thermal mode	Adiabatic	–
HDO pressure	40	bar
HDO lipid:H_2 ratio	97.13/2.87	w%
HDO retention time	1	h
HDO exit temperature	100	°C
Flash 1 temperature	50	°C
Flash 1 pressure	1	bar
Decanter water separation	100	w%
HI input temperature	250	°C
HI thermal mode	Adiabatic	–
HI pressure	30	bar
HI n-alkane:H_2 ratio	96.50/3.50	w%
HI retention time	1	h
HI exit temperature	227	°C
Fuel distillation (Fig. 15)		
Flash 2 temperature	35	°C
Flash 2 pressure	1	bar
1st distillation tower temperature	190	°C
2nd distillation tower temperature	218.5	°C

Table 8
Input data for material and chemical costs.

Parameter	Value [USD kg^{-1}]	Ref.
Buying prices		
Salicornia sp.	0[a]	–
Hydrogen	2.00	[6]
Reaction water	0.0025	[45]
Cellulase	0.50	[46]
CF	0.55	[23]
EtOH	8.56	[47]
N-hexane	12.75	[47]
Steam (152 °C)	0.012	SPD
Process cooling water (25–30 °C)	0.00005	SPD
Electricity	0.1[b]	SPD
Selling prices		
Salicornia sp. lipids	1.00[a]	–
Salicornia sp. EtOH extract	7.00	[48]
Frass	2.00	[49]
BSFL screw-pressed cake	0.72	[23]
BSFL protein	2.17	[23]
BSFL lipids	0.30[a]	–
Hydrogen	2.00	[6]
Propane	0.80	[6]
Naphta range fuel	0.55	[6]
HEFA-SPK range fuel	0.62	[6]
HVO range fuel	1.00	[6]

[a] Assumption.
[b] USD kWh^{-1}.

of the bacterial culture self-sustainable due to *in situ* production. The price of the raw input biomass, *Salicornia* sp., is thought to be free, as the biomass is a waste product after food production, and producers are considering it as a waste product [48]. The cost of cellulase is based on an optimization research from by Kadhum et al. [46].

Table 9 shows the stoichiometric reactions included in the biorefinery model simulation.

2.10. Biorefinery section optimization

In order to successfully determine the possible gains or losses affiliated by each processing section, Figs. 7–15, were tested in different

Table 9
All possible reactions with their respective stoichiometric coefficients.

Reaction	Stoichiometry	Type
	Hydrodeoxygenation reactor	
1	$3\ m \cdot H_2 + 1\ tri{-}C_{18:m} \rightarrow 1\ tri{-}C_{18:0}$	Molar
2,3,5	$6\ H_2 + tri{-}C_{n:0} \rightarrow 3\ CO + 3\ C_{(n-1)}H_{2(n-1)+2} + C_3H_8 + 3\ H_2O$	Molar
2,3,6,7	$12\ H_2 + tri{-}C_{n:0} \rightarrow 3\ C_nH_{2n+2} + C_3H_8 + 6\ H_2O$	Molar
2,4	$3\ H_2 + tri{-}C_{n:0} \rightarrow 3\ CO_2 + 3\ C_{(n-1)}H_{2(n-1)+2} + C_3H_8$	Molar
	HI reactor	
8	$H_2 + C_nH_{2n+2} \rightarrow C_{n-3}H_{2(n-3)+2} + C_3H_8$	Molar
9	$H_2 + C_nH_{2n+2} \rightarrow C_{n-8}H_{2(n-8)+2} + C_8H_{18}$	Molar
10	$H_2 + C_nH_{2n+2} \rightarrow C_{n-7}H_{2(n-7)+2} + C_7H_{16}$	Molar
11	$H_2 + C_{18}H_{38} \rightarrow 2\ C_9H_{20}$	Molar
11	$H_2 + C_{16}H_{34} \rightarrow 2\ C_8H_{18}$	Molar
12	$C_nH_{2n+2} \rightarrow i{-}C_nH_{2n+2}$	Molar
	Generic boxes	
13	$100\ fermented\ feed \rightarrow 0.93\ NH_3 + 11.83\ BSFL + 8.00\ residue + 4.56\ frass + 74.68\ H_2O$	Mass
14	$100\ BSFL \rightarrow 22.54\ BSFL\ lipid + 32.00\ protein + 45.46\ residue$	Mass
15	$100\ BSFL\ lipid \rightarrow 39.4\ tri{-}C_{12:0} + 7.6\ tri{-}C_{14:0} + 18.6\ tri{-}C_{16:0} + 5.0\ tri{-}C_{18:0} + 23.6\ tri{-}C_{18:1} + 5.8\ tri{-}C_{18:2}$	Mass

Table 10
Simulated process sections to determine the benefit of extra processing. Numbers in the table refer to Figs. 7–15.

Process description	Figures
Salicornia sp. extract	7–9
Salicornia sp. extract and BSFL products	7–13
Full simulation	7–15

Table 11
Characterization of *Salicornia* sp. pulp and BSFL used for simulation. n/a: not available.

Compound	*Salicornia* sp. pulp [w%]	BSFL [w%]
Water	86.39	61.45
Dry matter		
Lipids	6.64	22.54
EtOH solubles		
- Ash	5.53	n/a
- Others	3.32	n/a
Protein	10.92	32.00
Structural sugars		
- Arabinose	6.22	n/a
- Glucose	24.53	n/a
- Xylose	14.86	n/a
Lignin	14.19	n/a
Exoskeleton	n/a	9.00
Residue	13.79	36.46

scenarios, excluding specific processing sections. Table 10 shows different inclusion scenarios to be simulated, and analyzed for feasibility.

3. Results

This section describes the results reached from simulations done in SuperPro Designer and Aspen HYSYS. Water content and mass components of *Salicornia* sp. and BSFL are shown in Table 11.

3.1. Simulation results

HDO, DCO_2 and DCO reaction inputs and outputs are collected in Table 12, which show a large amount of H_2O and CO_2 being produced

Table 12
Mass balance of simulated HDO reactions.

Compound	In [w%]	Out [w%]
H_2	2.87	0.40
H_2O	–	8.73
CO	–	0.42
CO_2	–	6.21
C3	–	5.74
C11	–	11.21
C12	–	18.39
Tri-C12:0	38.27	–
C13	–	2.25
C14	–	3.65
Tri-C14:0	7.38	–
C15	–	5.69
C16	–	9.14
Tri-C16:0	18.07	–
C17	–	10.86
C18	–	17.32
Tri-C18:0	4.86	–
Tri-C18:1	22.92	–
Tri-C18:2	5.63	–

and a small amount of CO. An issue with co-producing oxocarbons is the impact of GHG emissions, as the production of biofuels should aim to reduce the overall emission of CO_2-equivalents. Another issue with the co-production of oxocarbons is the chemical energy in the carbon-bonds should preferably be used in combustion, rather than as an emitted co-product. Another gaseous co-product is propane. Most of the propane is flashed off with CO_2 and unreacted H_2, CO, H_2O and some of the heavy alkanes. The reason for the partial removal of heavy alkanes is due to the azeotropic properties of alkane mixtures. Of the flashed products after the HDO reactor, 0.26 w% is heavy alkanes. This amount can be decreased by lowering the flash temperature, thus also shifting the propane/heavy alkane azeotrope to include more propane in the fuel mixture.

Once reacted into n-alkanes, the stream is partially isomerized and hydrocracked into i-alkanes for fuel refinery. Table 13 shows the input and output mass balance. Due to a higher amount of lighter alkanes formed (C7–C10), the share of these in the flashed products will be higher, hence the temperature of the flash evaporation column is lowered to 35 °C (see Table 14).

The heavy key distillation temperature of Jet A-1 is set to be 220 °C, as it enables the separation of heavier hydrocarbons and yields the jet fuel product matching the ASTM standards. Distillation at higher temperatures results in the product including too many heavy alkanes, increasing the freezing point above the standardized limit of −47 °C. Table 15 shows the distribution of alkanes in the final distilled fuels.

3.2. Techno-economic assessment results

Using techno-economic assessment (TEA) sensitivity analysis, a range of input mass flow rates between 10–140 t h^{-1} has been chosen for the simulation. Shpigel et al. [15] has reported the yearly harvest of *Salicornia* sp. to be 26,000 kg fresh *Salicornia* sp. ha^{-1}. Of this amount, 8700 kg will be food grade biomass, and 17,300 kg will be residual biomass, corresponding to the biomass used for this simulation. SPD has a default operational up-time of 330 days, 7920 h, per year, for a process plant lifetime of 15 years. The biomass input mass flow rate of 10–140 t h^{-1} is thereby corresponding to the yearly harvest from 4580–64,090 ha, after the food grade biomass have been harvested. It should be noted that this land could be salt affected, and would therefore not compete with food production. Cultivation of 4580–64,090 ha *Salicornia* sp. might not be feasible for a small group of farmers, so the biomass for a biorefinery of said size could be distributed over a nation. As an input mass flow rate above 80 t h^{-1} is relatively large, the constraint of reactor and vessel volumes forces SPD to make parallel

Table 13
Mass balance of simulated HI reactions.

Compound	Input [w%]	Output [w%]
H_2	3.50	3.13
C3	0.64	5.14
C7	–	1.27
C8	–	0.71
i-C8	–	6.39
C9	–	0.74
i-C9	–	5.43
C10	–	0.54
i-C10	–	4.85
C11	13.66	2.03
i-C11	–	18.29
C12	22.45	2.57
i-C12	–	23.10
C13	2.75	0.58
i-C13	–	5.19
C14	4.46	1.76
i-C14	–	2.06
C15	6.95	2.77
i-C15	–	1.04
C16	11.16	4.71
i-C16	–	0.30
C17	13.27	3.51
i-C17	–	0.51
C18	21.15	2.76
i-C18	–	0.64

Table 14
Limits and common values for naphtha [43], HEFA-SPK [42] and HVO [43,50,51].

Parameter	Naphtha	HEFA-SPK	HVO	Unit
Limits/common values				
Freezing point	–	<−47.0	<−10.0	°C
Density at 15 °C	–	775–840	780–890	kg m^{-3}
Kinematic visc.	–	<8.0[a]	1.9–6.0[b]	mm^2 s^{-1}
Distillation temperature	70–180	>205–<300	240–340	°C
Simulated products				
Freezing point	−64.9	−47.1	−18.8	° C
Density at 15 °C	772.8	786.4	789.1	kg m^{-3}
Kinematic visc.	2.6[a]	4.2[a]	2.1[b]	mm^2 s^{-1}
Distillation temperature	<190	190–220	>220	°C

[a]Kinematic viscosity at −20 °C.
[b]Kinematic viscosity at 40 °C.

Table 15
Comparison of distilled fuel products from BSFL lipid based HI alkanes in kg h^{-1}. Biorefinery input mass flow rate of *Salicornia* sp. of 10 ton h^{-1}.

Alkane	Input	Naphtha	HEFA-SPK	HVO
C3	0.3	0.3	0	0
C7	2.1	1.7	0.4	0
C8	1.4	1.0	0.4	0
i-C8	14.3	10.0	4.0	0.3
C9	1.6	0.8	0.7	0.1
i-C9	11.8	6.8	4.4	0.6
C10	1.2	0.5	0.6	0.1
i-C10	10.8	4.9	4.9	1.0
C11	4.5	1.4	2.3	0.8
i-C11	40.9	13.9	20.6	6.4
C12	5.8	1.2	3.0	1.6
i-C12	51.8	12.7	26.6	12.5
C13	1.3	0.2	0.6	0.5
i-C13	11.7	2.0	5.7	4.0
C14	4.0	0.4	1.5	2.1
i-C14	4.6	0.5	2.0	2.1
C15	6.2	0.4	1.9	3.9
i-C15	2.3	0.2	0.8	1.3
C16	10.6	0.4	2.6	7.6
i-C16	0.7	0.1	0.2	0.4
C17	7.9	0.2	1.4	6.3
i-C17	1.1	0	0.3	0.8
C18	6.2	0.1	0.8	5.3
i-C18	1.4	0	0.3	1.1
Σ	204.6	59.5	86.1	59.0

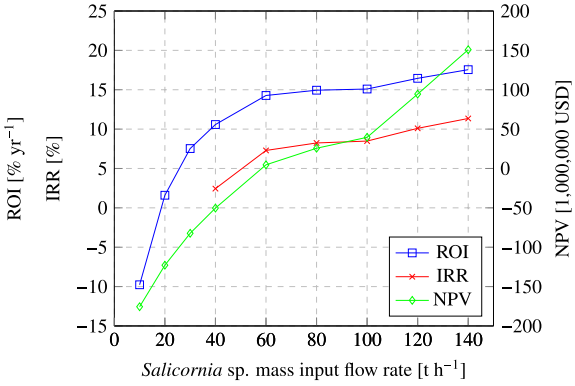

Fig. 4. Techno-economic assessment sensitivity analysis of the overall simulation. Parameters for techno-economic assessment includes return on investment, internal rate of return and net present value.

units. Due to parallel units being simulated, the capital expenditure (CAPEX) of the TEA is increased as the input mass flow rate exceeds a limit just above 80 t h^{-1}. Considering the return on investment (ROI), this creates a local optimum at 80 t h^{-1}, as seen on Fig. 4. The revenue streams from the biorefinery process includes *Salicornia* sp. revenue, BSFL revenue and fuel revenue. Of these revenue streams, a direct linear correlation to the input mass flow rate exists, meaning a 100% increase in input mass flow rate corresponds to a 100% increase in revenue. Expenses, CAPEX and operational expenditure (OPEX), are independent and do not show linear correlation to the input mass flow rate. This is as the price of the equipment follows a power law, e.g. the increase in cost of centrifugal pumps per unit of electrical power capacity, will decrease as the electrical power capacity increases.

Table 16 summarizes the throughput, retention time, and simulation purchase price of equipment, apart from transport, mixing and utility equipment at a mass flow rate of 10 t h^{-1}. As the mass flow rate was changed for sensitivity analysis, the throughput increased as a direct linear correlation to the mass flow rate. All units did not increase retention time, apart from an exponential increase in decanter retention time, which would exponentially increase the volume of said decanters due to the fluid properties of the decanted liquids. The parameters for a TEA was found using internal calculations from SPD. The TEA is dependent on multiple analysis parameters, and for this case, will include return on investment (ROI), internal rate of return after tax (IRR) and net present value at 7% interest rate (NPV). The reason for including multiple parameters in the TEA was due to the complexity of a financial investment of such size. For an investment to be deemed financially feasible, the ROI has to be larger than a certain threshold set by the investor. In this case, the threshold was set to be >10 % yr^{-1}. Furthermore, the NPV has to be positive over the process plant lifetime, as NPV is a measure of the total profit accounting for the interest rate, set by SPD, of 7% in present value, over the process plant lifetime, which was set to be 15 years. IRR is a measure of the maximum interest rate allowed for the process, allowing NPV = 0 after the process plant lifetime.

$$ROI = \frac{Net\ profit}{CAPEX} \tag{4}$$

$$NPV = \sum_{k=0}^{t} \frac{Net\ profit_t}{(107\%)^t} - CAPEX \tag{5}$$

Where t is the project lifetime in years, net $profit_t$ is the generated net profit in year t.

Table 16
Process sizing and cost at 10 t h^{-1}. Transport, mixing and utility equipment excluded.

Figure	Equipment	Throughput [kg h^{-1}]	Retention time [h]	Purchase price [1000 USD]
7	Screw press	10,000.0	1	274
7	Drum drier	1375.0	10	50
7	Shredder	1361.2	1	81
8	Extractor	14,735.1	2	44
8	Evaporator	14,735.1	1	23
8	Decanter	1495.0	0.006	34
8	Product storage	221.9	24	14
8	Solvent storage	13,373.9	24	267
9	Extractor	16,322.6	6	90
9	Evaporator	16,322.6	1	50
9	Decanter	1422.2	0.02	34
9	Product storage	270.4	24	13
9	Solvent storage	15,050.9	24	255
10	Pretreatment reactor	19,112.1	1.2	337
10	Storage	19,112.1	24	337
10	Hydrolysis reactor	19,194.5	24	304
10	Sludge drier	20,919.5	1	33
11	Batch storage	392.5	24	71
11	Batch seed fermentor	408.2	24	945
11	Storage	392.5	24	52
12	Blending/Storage	9825.9	30	307
12	Fermentor	10,218.4	26.5	2833
12	Feedstock storage	10,218.4	30	157
12	BSFL cultivation unit	9825.9	336	124
12	Fly reproduction unit	12.1	168	6
13	Frass storage	7006.8	24	107
13	Devitalization unit	3104.5	1	353
13	BSFL storage	3104.5	24	73
13	Screw press	3104.5	1	108
13	BSFL residue storage	3104.5	24	73
13	Decanter 1	2555.0	0.05	34
13	Decanter 2	2289.5	1.02	56
13	Drum drier	955.9	1.7	152
14	HDO reactor	274.3	1	71
14	Flash	274.3	5.4	2
14	Decanter	239.1	0.004	34
14	HI reactor	224.6	1	71
15	Flash	224.6	31.5	1
15	Naphtha storage	59.5	24	4
15	HEFA storage	86.1	24	3
15	HVO storage	59.0	24	4

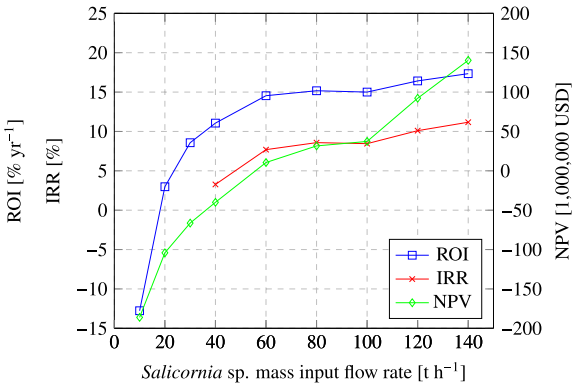

Fig. 5. Techno-economic assessment sensitivity analysis of simulation excluding biofuel production. Parameters for techno-economic assessment includes return on investment, internal rate of return and net present value.

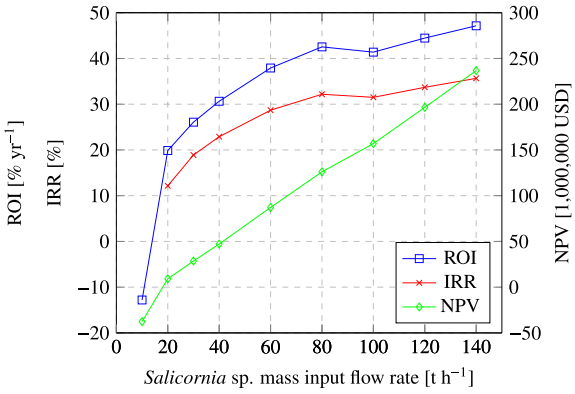

Fig. 6. Techno-economic assessment sensitivity analysis of simulation excluding BSFL refinery and biofuel production. Parameters for techno-economic assessment includes return on investment, internal rate of return and net present value.

Fig. 4 shows the techno-economic assessment parameters as the input mass flow rate of *Salicornia* sp. increases. ROI is above the set threshold of 10% at a input mass flow rate of >40 t h^{-1}, NPV is positive at a input mass flow rate input of >60 t h^{-1}. NPV shows a large increase at mass flow rates of >100 t h^{-1}. This increase is due to the larger revenue relative to OPEX, compared to lower input mass flow rates. The TEA parameters shows to be stable, with little increase, at mass flow rates of 60–100 t h^{-1}. This is due to the volume constraints from many of the operational units in SPD, as SPD will force the simulation of multiple parallel smaller units (see Table 17).

3.3. Process optimization

The feasibility of the three simulation scenarios specified in Table 10, were simulated individually, for a *Salicornia* sp. mass flow rate of 10–140 t h^{-1}. These were simulated for comparison and with the objective of identifying the most feasible of the simulated processes. The feasibility of the processes were interpreted from the financial analysis parameters.

Excluding processing of BSFL and jet-fuel shows to have a larger financial benefit, compared to inclusion of said processes, as seen from Figs. 4–6. A positive NPV can be achieved at a lower input mass flow rate of *Salicornia* sp. excluding processing of BSFL and biofuels. Furthermore, with a *Salicornia* sp. mass flow rate of 140 t h^{-1} an increase in biofuel prices of 20% will yield a minor increase of the ROI from 17.55% to 17.79%, IRR from 11.35 to 11.60% and NPV from 150,835,000 to 160,573,000 USD. This implies the majority of the profits are not generated by the production of biofuels, as the product of highest revenue is the ethanolic extract.

3.4. Energy and carbon dioxide assessment

For the production of biofuels, the amount of energy released as heat by combustion of biofuels should exceed the amount of energy used as electricity for the production of the biofuel. Likewise, the amount of net-CO_2 emitted by combustion of fossil fuels should be higher than the CO_2 emitted by the production of sustainable biofuels. The energy and net-CO_2 balances for each of the subdivided production steps was analyzed, and the potential energy released by stoichiometric combustion of the produced naphtha, HEFA-SPK, HVO and flashed propane was evaluated. Biofuel energy release was calculated using the lower heating value (LHV) of the fuel [52–55]. Furthermore, to evaluate the CO_2-equivalent (CO_2-e) cost of production compared to reduced CO_2 emission by biofuel combustion, the CO_2-e balance was calculated on a basis of production in Table 18, and on a basis of product in Table 19. The CO_2 reduction ratio, compared to CO_2 emitted by fossil fuels, was assessed. CO_2 emitted by electricity power production in Denmark was in 2018 on average 306 g kWh^{-1}, and CO_2 emitted by stoichiometric combustion of gasoline, jet-fuel, diesel

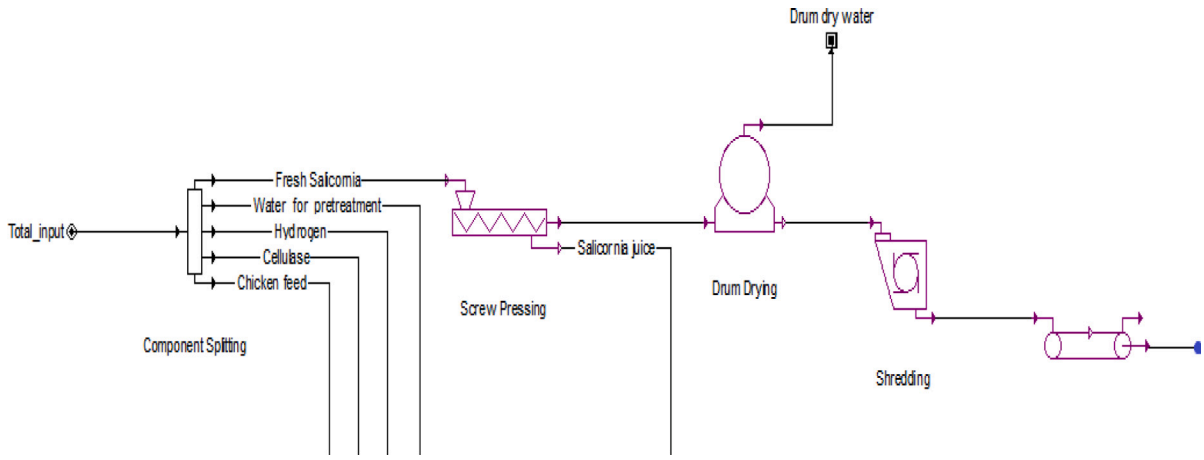

Fig. 7. 1: Preprocessing of *Salicornia* sp.

Table 17
Table of expense and revenue streams. In 1000 USD yr^{-1}.

Parameter	Input mass flow rate [t h^{-1}]									
	10	20	30	40	60	80	90	100	120	140
CAPEX	103,316	139,572	172,420	203,179	260,212	345,672	398,223	441,658	496,858	556,182
OPEX	45,232	62,097	80,227	97,968	132,199	172,563	193,671	227,152	248,522	282,693
***Salicornia* sp. revenue**										
Lipids	709	1418	2127	2836	4254	5672	6381	7090	8508	9926
EtOH extract	66,729	133,458	200,187	266,916	400,374	533,832	600,561	667,290	800,748	934,206
BSFL revenue										
Frass	7381	14,762	22,143	29,524	44,286	59,048	66,429	73,810	88,572	103,334
Screw press residue	3177	6354	9531	12,708	19,062	25,416	28,593	31,770	38,124	44,478
Protein	6568	13,136	19,704	26,272	39,408	52,544	59,112	65,680	78,816	91,952
Fuel revenue										
Flash 1	108	216	324	432	648	864	972	1080	1296	1512
Flash 2	183	366	549	732	1098	1464	1647	1830	2196	2562
Naphtha	259	518	777	1036	1554	2072	2331	2590	3108	3626
HEFA-SPK	423	846	1269	1692	2538	3384	3807	4230	5076	5922
HVO	467	934	1401	1868	2802	3736	4203	4670	5604	6538

Table 18
Energy and CO_2 balance at a input mass flow rate of 10 ton h^{-1}.

Process	Power [kWh h^{-1}]	Net-CO_2-e emitted [kg h^{-1}]
Energy expense		
H_2 production	409.6	125.3
1	42.0	12.9
2	125.7	38.5
3	153.0	46.8
4	4.2	1.3
5	3.1	1.0
6	47.4	14.5 + 20.5[a]
7	7.2	2.2
8	107.5	32.9 + 18.7[b]
9	30.7	9.4
Σ	930.4	323.9
Produced fuels	2574.9	323.9
Equivalent fossil fuels	2574.9	659.5

[a]From the global warming potential of the biogenic emissions by BSFL assuming a feedstock carbon-to-nitrogen level of 25 [56].
[b]From the global warming potential of the produced oxocarbons [57].

Table 19
Net-CO_2-e emitted per unit of product.

Product	Processes	Net-CO_2-e emitted per product [kg CO_2-e kg^{-1}]
Salicornia sp. lipid	2	0.43
Salicornia sp. EtOH extract	3	0.39
BSFL frass	4–7	0.03
BSFL screw press residue	4–7	0.02
BSFL protein	4–7	0.04
Flash 1	8–9	0.35
Flash 2	8–9	0.61
Naphtha	8–9	0.21
HEFA-SPK	8–9	0.14
HVO	8–9	0.21

and propane, based on lower heating values, 259.3 g CO_2 kWh^{-1}, 257.5 g CO_2 kWh^{-1}, 258.9 g CO_2 kWh^{-1} and 240.2 g CO_2 kWh^{-1} respectively [58]. The produced biofuels are assumed to have similar molecular composition as their respective fossil fuel counterparts, and the combustion will therefore release the same amount of CO_2, with 3.17, 3.11, and 3.07 kg CO_2 per kg naphtha, HEFA-SPK and HVO respectively [58]. Most energy consumption of the process equipment was calculated by SPD as a function of mass flow rate and retention time in the equipment. The energy usage for the process equipment that could not be calculated by SPD was calculated using a technical report made by NREL [59]. As the HDO reactor emitted CO_2 and CO directly due to DCO_2 and DCO, this is also included in the CO_2-e balance.

To be able to determine the real net-CO_2-e emitted by the process and production of advanced biofuels, the emissions of co-products were calculated and normalized. Normalization of emissions expressed per unit of product will allow a process designer to determine the actual emitted net-CO_2-e per mass unit of biofuel.

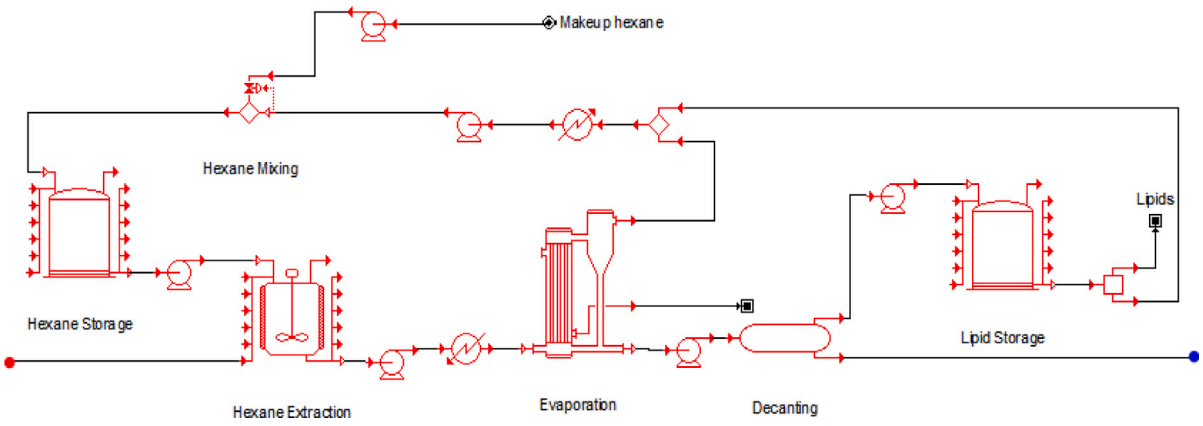

Fig. 8. 2: N-hexane Soxhlet extraction. Input from Fig. 7.

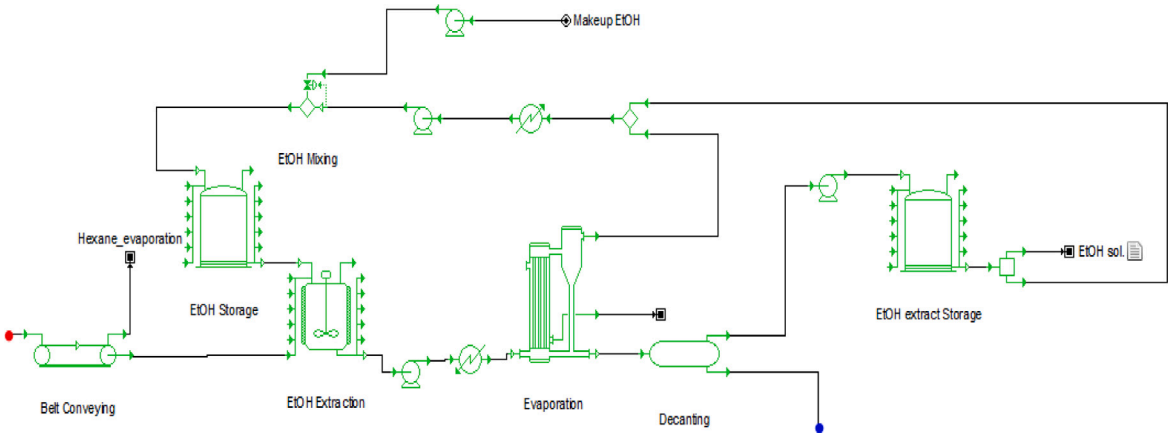

Fig. 9. 3: Ethanol Soxhlet extraction. Input from Fig. 8.

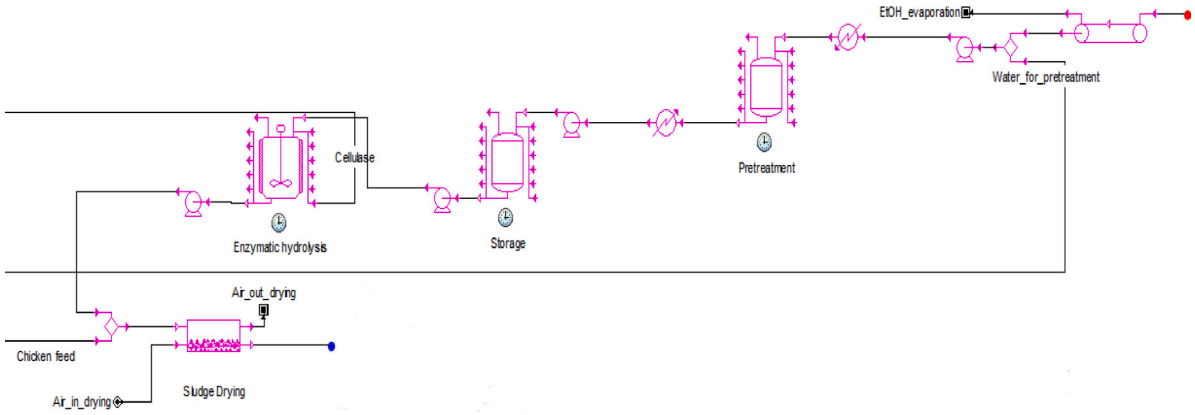

Fig. 10. 4: Hydrothermal pretreatment and enzymatic hydrolysis of extractive free lignocellulosic *Salicornia* sp. Input from Fig. 9.

From Table 18 it can be seen the simulated production of biofuels and co-products from *Salicornia* sp. and *Salicornia* sp. fed BSFL emits a net-amount of 323.9 kg CO_2 h^{-1}, whereas the combustion of the similar fuel, excluding production and refining energy expenses, emits a net-amount of 659.5 kg CO_2 h^{-1}. This carbon emission can be lowered by utilizing excess power production by either photovoltaic or wind energy. Combustion of these simulated produced biofuels yields an estimated net-CO_2-e reduction of 50.8%, with the co-production of terrestrial animal protein and EtOH extract with high bioactivity. Furthermore, the produced biofuel holds 276.8% of the energy required

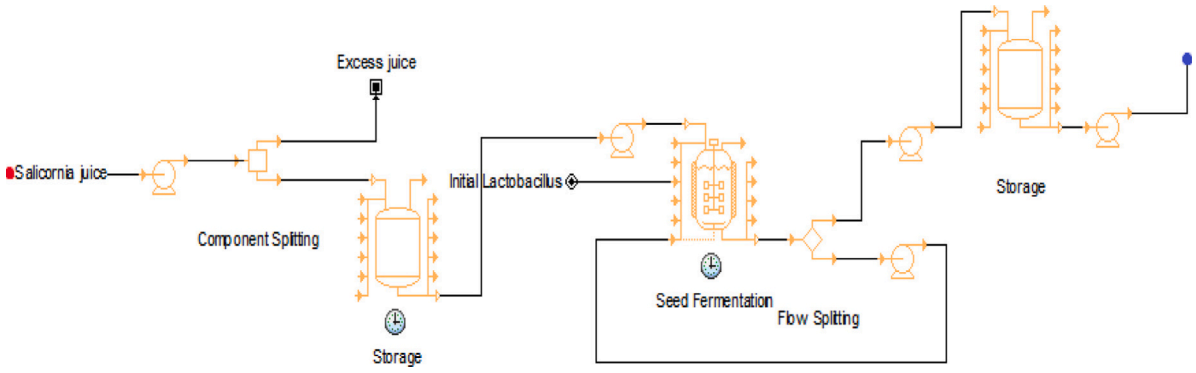

Fig. 11. 5: *Lactiplantibacillus plantarum* cultivation in *Salicornia* sp. juice. Input from Fig. 7.

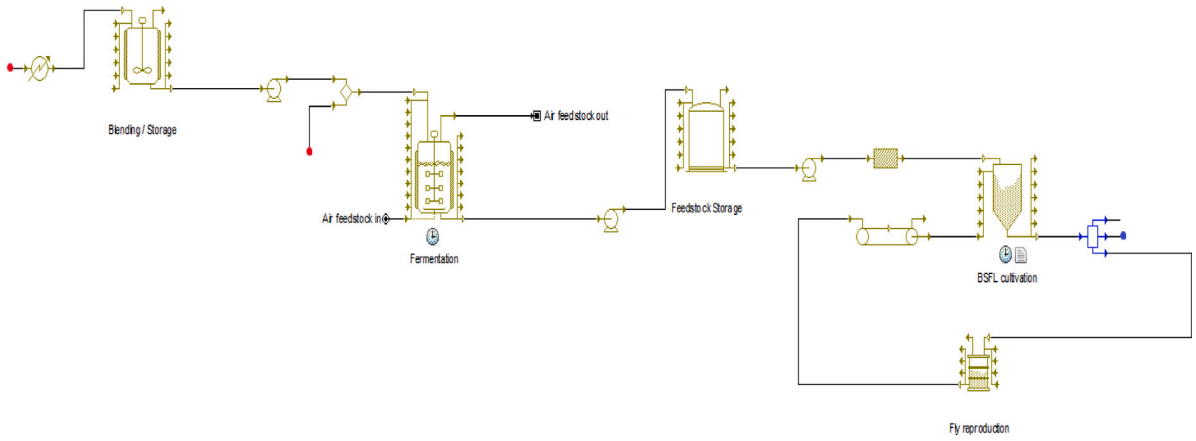

Fig. 12. 6: BSFL feedstock fermentation and BSFL cultivation. Input from Figs. 10 and 11.

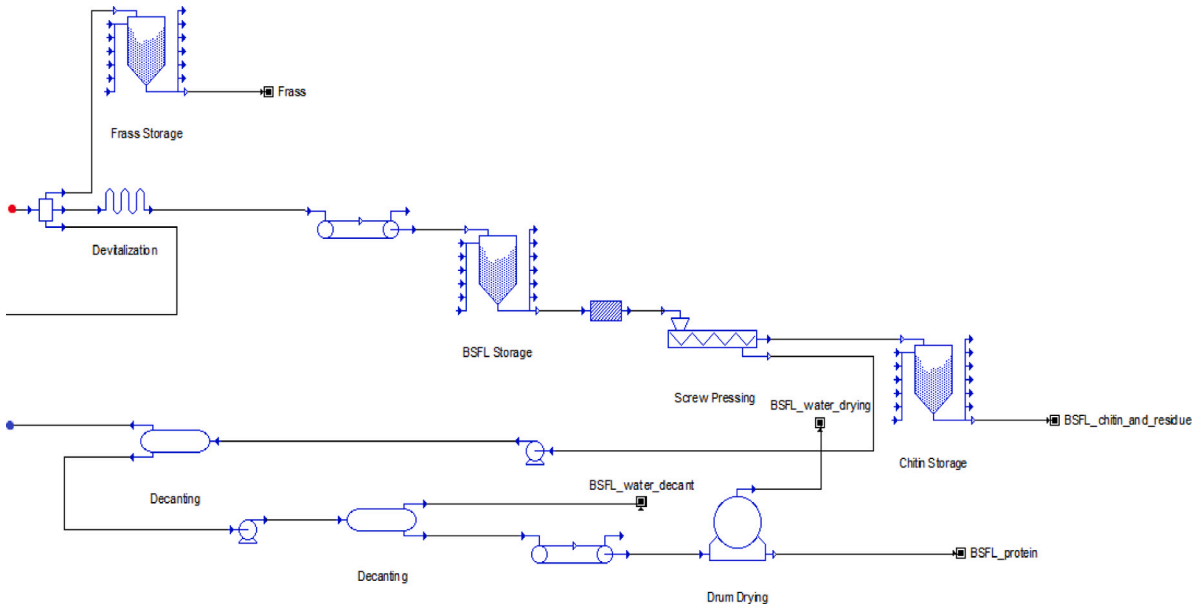

Fig. 13. 7: BSFL processing. Input from Fig. 12.

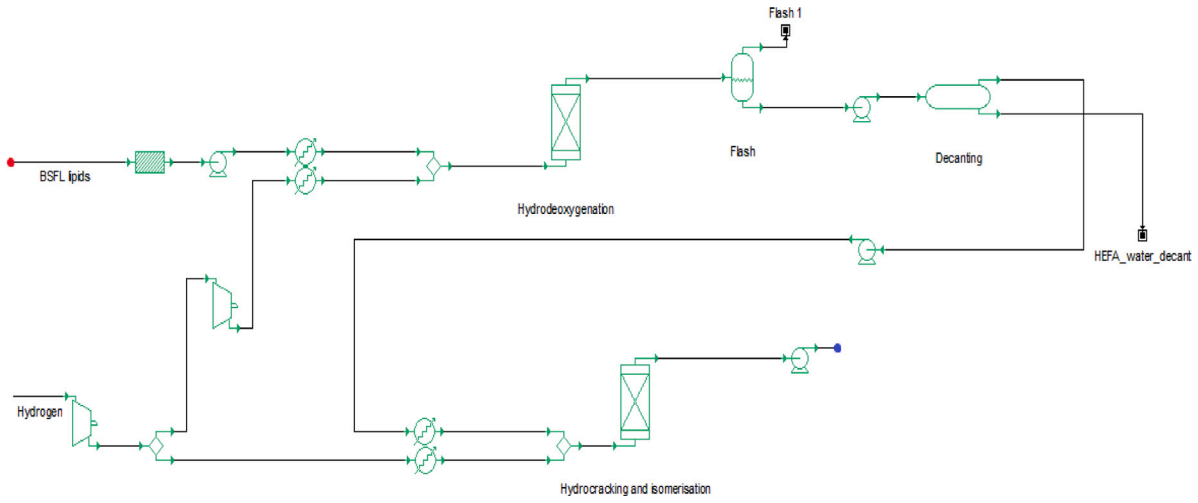

Fig. 14. 8: BSFL lipid hydrodeoxygenation and HI. Input from Fig. 13.

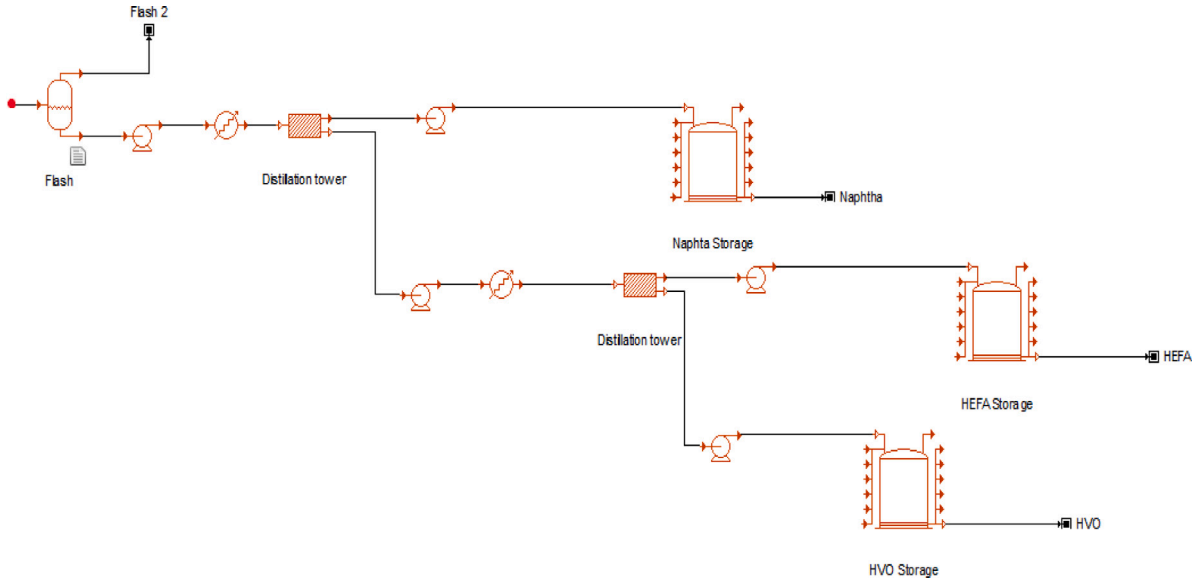

Fig. 15. 9: Fuel distillation. Input from Fig. 14.

for the process itself. Regarding the normalized net-CO_2-e emitted, the net-CO_2-e reduction of the naphtha, HEFA-SPK and HVO are 93.4%, 95.5% , 93.2% respectively.

4. Discussion

Most implemented advanced bio-fuels such as HEFA-SPK or Fischer Tropsch-SPK use excess biomass from food crops, hence being 1st generation bio-fuel. Some of this biomass comes from unsustainable sources as results of deforestation, extensive agricultural exploitation or production of high yielding lipid or sugar crops for the sole purpose of production of bio-fuels [60]. Cultivation of high-energy crops utilizes arable land for production of energy. This poses a dilemma where arable land and clean water are scarce resources, as cultivation of crops for bio-fuels may reduce the food production [61]. Traditional 2nd generation bio-fuels are typically produced from waste biomass that can require energy-intensive pretreatments to be able to break the lignocellulosic structure, as the lignin content of these types of biomass usually are relatively high, e.g. straw. Pretreatment of biomass will increase the amount of toxic furanic compounds and carboxylic acids, that could lead to poisoning of organisms used down-stream in the process [62]. The described process of *Salicornia* sp. biorefinery differs from other 2nd generation biorefineries, as the characterized *Salicornia* sp. contains very low lignin content, and extensive pretreatment is therefore not necessary prior to enzymatic hydrolysis. Furthermore, co-products such as low-CO_2 impact terrestrial animal protein and high value bioactive extract are produced from the process. BSFL protein are deemed low-impact CO_2-e protein, as the CO_2-e emitted per kg DM of BSFL can be 0.9–8.8% compared to traditional composting of similar feedstock, dependent on the carbon-to-nitrogen level of the feedstock which makes BSFL excellent low-CO_2-e impact food waste bioconverters, with the frass having good fertilizing properties [56]. Furthermore, the direct production of BSFL emits 0.14% CO_2-e per kg of BSFL compared to the CO_2-e intensive production of cattle carcass [63].

5. Conclusions

This paper has presented a full biorefinery process of *Salicornia* sp. to jet-fuel. *Salicornia* sp. was fractionated into lipids, valuable ethanol extracted phytochemicals, and excess extractive-free biomass. The excess extractive-free biomass was then simulated to be hydrothermally pretreated and enzymatically hydrolyzed, mixed with chicken feed, and fermented with *in situ* produced *Lactiplantibacillus plantarum*. *Hermetia illucens*, black soldier fly larvae, was added to the mixture of feedstock,

and devitalized after 14 days. Frass, protein and residual biomass from the BSFL were separated into fractions, and sold as co-products. The lipids from BSFL fractionation were processed into biofuels using hydrodeoxygenation, hydrocracking and isomerization over packed bed reactors.

Frass, protein from BSFL, and EtOH extract from *Salicornia* sp. were found to be the co-products with the highest product price, necessary to reach feasibility of the production of low normalized CO_2-e biofuels. Co-production of high-value compounds is crucial to reach feasibility in a biofuel refinery, as the value of fuel is drastically lower than the value of some of the co-products presented in this paper.

From this simulation, the optimized production of HEFA-SPK is deemed feasible and profitable, and needs to be shown on a pilot scale for complete mass balance, economic and emissions verification.

Acknowledgments

The authors thank Julaine Tania Enas for laboratory assistance and technical analysis. Furthermore, as feeding trials of BSFL were done by Enorm Biofactory A/S on site, the authors thank Enorm Biofactory A/S for the cooperation.

References

[1] EU, Flightpath 2050, Technical Report, European Union, Luxembourg, 2011.
[2] Boeing, Current Market Outlook 2016 – 2035, Technical Report, Seattle, 2016, pp. 1–54, URL https://www.boeing.com/resources/boeingdotcom/commercial/about-our-market/assets/downloads/cmo_print_2016_final_updated.pdf.
[3] Jane O'malley, Nikita Pavlenko, Stephanie Searle, Estimating sustainable aviation fuel feedstock availability to meet growing European Union demand, Technical Report, 2021, URL www.theicct.org.
[4] Seamus J Bann, Robert Malina, Mark D Staples, Pooja Suresh, Matthew Pearlson, Wallace E Tyner, James I Hileman, Steven Barrett, The costs of production of alternative jet fuel: A harmonized stochastic assessment, Bioresour. Technol. 227 (2017) 179–187.
[5] Wei-Cheng Wang, Ling Tao, Jennifer Markham, Yanan Zhang, Eric Tan, Liaw Batan, Ethan Warner, Mary Biddy, Review of biojet fuel conversion technologies, 2016, URL www.nrel.gov/publications.
[6] E Martinez-Hernandez, Lf Ramirez-Verduzco, MA Amezcua-Allieri, J Aburto, Process simulation and techno-economic analysis of bio-jet fuel and green diesel production - minimum selling prices, Chem. Eng. Res. Des. 146 (2019) 60–70.
[7] Lucile Chatellard, Amandine Gales, Adèle Lazuka, Lucas Auer, Maider Abadie, Hélène Carrère, Jean-Jacques Godon, Michael O'Donohue, Guillermina Hernandez Raquet, Claire Dumas, Biomimetic approach for developing lignocellulose valorization bioprocess using insect microbiome, in: World Congress on Anaerobic Digestion, 2015.
[8] Qing Li, Longyu Zheng, Ning Qiu, Hao Cai, Jeffery K Tomberlin, Ziniu Yu, Bioconversion of dairy manure by black soldier fly (diptera: Stratiomyidae) for biodiesel and sugar production, Waste Manag. 31 (6) (2011) 1316–1320.
[9] Xiaopeng Xiao, Lorenzo Mazza, Yongqiang Yu, Minmin Cai, Longyu Zheng, Jeffery K Tomberlin, Jeffrey Yu, Arnold van Huis, Ziniu Yu, Salvatore Fasulo, Jibin Zhang, Efficient co-conversion process of chicken manure into protein feed and organic fertilizer by hermetia illucens l. (diptera: Stratiomyidae) larvae and functional bacteria, J. Environ. Manag. 217 (2018) 668–676.
[10] Moritz Gold, Jeffery K Tomberlin, Stefan Diener, Christian Zurbrügg, Alexander Mathys, Decomposition of biowaste macronutrients, microbes, and chemicals in black soldier fly larval treatment: A review, Waste Management 82 (2018) 302–318.
[11] Franklin B Apea-Bah, Amanda Minnaar, Megan J Bester, Kwaku G Duodu, Sorghum–cowpea composite porridge as a functional food, part II: Antioxidant properties as affected by simulated in vitro gastrointestinal digestion, Food Chem. 197 (Pt A) (2016) 307–315.
[12] Ni Du, Shuwen Cao, Yanying Yu, Research on the adsorption property of supported ionic liquids for ferulic acid, caffeic acid and salicylic acid, Journal of Chromatography B 879 (19) (2011) 1697–1703.
[13] Govindarajan Karthivashan, Mee-Hyang Kweon, Shin-Young Park, Joon-Soo Kim, Deuk-Hoi Kim, Palanivel Ganesan, Dong-Kug Choi, Cognitive-enhancing and ameliorative effects of acanthoside b in a scopolamine-induced amnesic mouse model through regulation of oxidative/inflammatory/cholinergic systems and activation of the trkb/CREB/BDNF pathway, Food Chem. Toxicol. 129 (2019) 444–457.
[14] Elisiário J Tavares-Da-Silva, Carla L Varela, Ana S Pires, João C Encarnação, Ana M Abrantes, Maria F Botelho, Rui A Carvalho, Carina Proença, Marisa Freitas, Eduarda Fernandes, Fernanda M.F Roleira, Combined dual effect of modulation of human neutrophils' oxidative burst and inhibition of colon cancer cells proliferation by hydroxycinnamic acid derivatives, Bioorganic & Medicinal Chemistry 24 (16) (2016) 3556–3564.
[15] M. Shpigel, D. Ben-Ezra, L. Shauli, M. Sagi, Y. Ventura, T. Samocha, J.J. Lee, Constructed wetland with salicornia as a biofilter for mariculture effluents, Aquaculture 412–413 (2013) 52–63.
[16] Yvonne Ventura, Wegi A. Wuddineh, Malika Myrzabayeva, Zerekbay Alikulov, Inna Khozin-Goldberg, Muki Shpigel, Tzachi M. Samocha, Moshe Sagi, Effect of seawater concentration on the productivity and nutritional value of annual salicornia and perennial sarcocornia halophytes as leafy vegetable crops, Sci. Hortic. 128 (3) (2011) 189–196.
[17] M.D Luque de Castro, F Priego-Capote, Soxhlet extraction: Past and present panacea, J. Chromatogr. A 1217 (16) (2009) 2383–2389.
[18] A Sluiter, B Hames, R Ruiz, C Scarlata, J Sluiter, D Templeton, Determination of Ash in Biomass: Laboratory Analytical Procedure (LAP); Issue Date: 7/17/2005, Technical Report, 2008, URL www.nrel.gov.
[19] Manish Kumar Patel, Sonika Pandey, Harshad R Brahmbhatt, Avinash Mishra, Bhavanath Jha, Lipid content and fatty acid profile of selected halophytic plants reveal a promising source of renewable energy, Biomass Bioenergy 124 (2019) 25–32.
[20] Donghe Lu, Min Zhang, Shaojin Wang, Jinlong Cai, Xiang Zhou, Chengpei Zhu, Nutritional characterization and changes in quality of salicornia bigelovii torr. during storage, LWT - Food Sci. Technol. 43 (3) (2010) 519–524.
[21] R.D Etheridge, G.M Pesti, E.H Foster, A comparison of nitrogen values obtained utilizing the kjeldahl nitrogen and dumas combustion methodologies (leco CNS 2000) on samples typical of an animal nutrition analytical laboratory, Anim. Feed Sci. Technol. 73 (1–2) (1998) 21–28.
[22] David W. Templeton, Lieve M.L. Laurens, Nitrogen-to-protein conversion factors revisited for applications of microalgal biomass conversion to food, feed and fuel, Algal Res. 11 (2015) 359–367.
[23] Enorm Biofactory A/S, Interview with lasse hinrichsen, 2019.
[24] Ayah Alassali, Iwona Cybulska, Alejandro Rí os Galvan, Mette Hedegaard Thomsen, Wet fractionation of the succulent halophyte salicornia sinus-persica, with the aim of low input (water saving) biorefining into bioethanol, Appl. Microbiol. Biotechnol. 101 (2017).
[25] Chuanji Fang, Jens Ejbye Schmidt, Iwona Cybulska, Grzegorz P. Brudecki, Christian Grundahl Frankær, Mette Hedegaard Thomsen, Hydrothermal pretreatment of date palm (l.) leaflets and rachis to enhance enzymatic digestibility and bioethanol potential, BioMed Res. Int. 2015 (2015) 13.
[26] Muhammad Tahir Ashraf, Mette Hedegaard Thomsen, Jens Ejbye Schmidt, Hydrothermal pretreatment and enzymatic hydrolysis of mixed green and woody lignocellulosics from arid regions, Bioresour. Technol. 238 (2017) 369–378.
[27] Sigma-Aldrich, Cellulase aqueous solution, more than 700units/g | 9012-54-8 | sigma-aldrich, 2020, URL https://www.sigmaaldrich.com/catalog/product/sigma/c2730?lang=en&region=DK.
[28] B Adney, J Baker, Measurement of Cellulase Activities: Laboratory Analytical Procedure (LAP); Issue Date: 08/12/1996, Technical Report, 1996, URL www.nrel.gov.
[29] Medana Zamfir, Silvia Grosu-Tudor, Impact of stress conditions on the growth of lactobacillus acidophilus IBB 801 and production of acidophilin 801, J. Gen. Appl. Microbiol. 55 (4) (2009) 277–282.
[30] G. Melgar-Lalanne, Y. Rivera-Espinoza, R. Farrera-Rebollo, H. Hernández-Sánchez, Survival under stress of halotolerant lactobacilli withprobiotic properties, Rev. Mex. Ing. Quím. 13 (1) (2014) 323–335.
[31] Qing Li, Longyu Zheng, Hao Cai, E Garza, Ziniu Yu, Shengde Zhou, From organic waste to biodiesel: Black soldier fly, hermetia illucens, makes it feasible, Fuel (Guildford) 90 (4) (2011) 1545–1548.
[32] L.J. Swicklik, C.A. Hollingsworth, B.F. Daubert, The kinetics of the hydrogenation of triglycerides, J. Amer. Oil Chem. Soc. 32 (2) (1955) 69–73.
[33] A.K Sinha, M Anand, S.A Farooqui, Chapter 5 - aviation biofuels through lipid hydroprocessing, in: Biofuels for Aviation, Elsevier Inc, 2016, pp. 85–108.
[34] Prakhar Arora, Eva Lind Grennfelt, Louise Olsson, Derek Creaser, Kinetic study of hydrodeoxygenation of stearic acid as model compound for renewable oils, Chem. Eng. J. 364 (2019) 376–389.
[35] Praepilas Dujjanutat, Pakawadee Kaewkannetra, Production of bio-hydrogenated kerosene by catalytic hydrocracking from refined bleached deodorised palm/palm kernel oils, Renew. Energy 147 (P1) (2020) 464–472.
[36] Zoltán Eller, Zoltán Varga, Jen˝ o Hancsók, Advanced production process of jet fuel components from technical grade coconut oil with special hydrocracking, Fuel 182 (2016) 713–720.
[37] Rogelio Sotelo-Boyas, Yanyong Liu, Tomoaki Minowa, Renewable diesel production from the hydrotreating of rapeseed oil with pt/zeolite and nimo/Al2o3 catalysts, Ind. Eng. Chem. Res. 50 (5) (2011) 2791–2799.
[38] Yanyong Liu, Rogelio Sotelo-Boyas, Kazuhisa Murata, Tomoaki Minowa, Kinya Sakanishi, Hydrotreatment of vegetable oils to produce bio-hydrogenated diesel and liquefied petroleum gas fuel over catalysts containing sulfided Ni–mo and solid acids, Energy Fuels 25 (10) (2011) 4675–4685.
[39] Il-Ho Choi, Kyung-Ran Hwang, Jeong-Sik Han, Kyong-Hwan Lee, Ji Sun Yun, Jin-Suk Lee, The direct production of jet-fuel from non-edible oil in a single-step process, Fuel 158 (2015) 98–104.
[40] R.A. Flinn, O.A. Larson, Harold Beuther, The mechanism of catalytic hydrocracking, Ind. Eng. Chem. 52 (2) (1960) 153–156.

[41] H.L Coonradt, W.E Garwood, Mechanism of hydrocracking. Reactions of paraffins and olefins, Ind. Eng. Chem. Process Des. Dev. 3 (1) (1964) 38–45.
[42] Starck Laurie, Pidol Ludivine, Jeuland Nicolas, Chapus Thierry, Bogers Paul, Bauldreay Joanna, Production of hydroprocessed esters and fatty acids (HEFA) – optimisation of process yield, Oil Gas Sci. Technol. 71 (1) (2016) 10.
[43] William Leffler, Fundamentals of Petroleum Refining, fourth ed., PennWell, Tulsa, Oklahoma, 2009, pp. 69–83.
[44] Hjelm Media Group AB, Lønstatistik, 2021, URL https://www.lonstatistik.dk/lonninger.asp?job=Procesoperator-4416.
[45] Trefor, Priser p vand, 2020, URL https://trefor.dk/vand/vandpriser-og-politikker.
[46] Haider Jawad Kadhum, Karthik Rajendran, Ganti S Murthy, Optimization of surfactant addition in cellulosic ethanol process using integrated techno-economic and life cycle assessment for bioprocess design, ACS Sustain. Chem. Eng. 6 (11) (2018) 13687–13695.
[47] Julaine Tania Enas, Laboratory chemicals price, 2019.
[48] Mette Hedegaard Thomsen, Integrated on-Farm Aquaponics Systems for Co-Production of Fish, Halophyte Vegetables, Bioactive Compounds, and Bioenergy, Technical report, Aalborg University, Esbjerg, 2019.
[49] KIS Organics, Natural insect fertilizer (frass) 3-2-4, 2021, URL https://www.kisorganics.com/products/natural-insect-fertilizer-frass?variant=22563599425.
[50] Jieni Wang, Weina Zhao, Yani Ai, Hongyan Chen, Leichang Cao, Sheng Han, Improving the fuel properties of biodiesel via complementary blending with diesel from direct coal liquefaction, RSC Adv. 5 (56) (2015) 45575–45581.
[51] J.K. Satyarthi, T. Chiranjeevi, D.T. Gokak, P.S. Viswanathan, An overview of catalytic conversion of vegetable oils/fats into middle distillates, Catal. Sci. Technol. 3 (1) (2012) 70–80.
[52] David Chiaramonti, Matteo Prussi, Marco Buffi, Daniela Tacconi, Sustainable bio kerosene: Process routes and industrial demonstration activities in aviation biofuels, Appl. Energy 136 (2014) 767–774.
[53] Lucimar Venâncio Amaral, Nathália Duarte Souza Alvarenga Santos, Vinícius Rückert Roso, Rita de Cássia de Oliveira Sebastião, Fabrício José Pacheco Pujatti, Effects of gasoline composition on engine performance, exhaust gases and operational costs, Renew. Sustain. Energy Rev. 135 (2021) 110196.
[54] Seok Hwan Lee, Jack J. Yoh, Investigation of hydrogen and electrolytic oxy-hydrogen addition to propane flames using planar laser-induced fluorescence, Fuel 183 (2016) 593–600.
[55] Magí n Lapuerta, Monserrat Villajos, John R. Agudelo, André L. Boehman, Key properties and blending strategies of hydrotreated vegetable oil as biofuel for diesel engines, Fuel Process. Technol. 92 (12) (2011) 2406–2411.
[56] Wancheng Pang, Dejia Hou, Elhosseny E. Nowar, Huanchun Chen, Jibin Zhang, Guoping Zhang, Qing Li, Shucai Wang, The influence on carbon, nitrogen recycling, and greenhouse gas emissions under different c/n ratios by black soldier fly, Environ. Sci. Pollut. Res. 27 (34) (2020) 42767–42777.
[57] John S. Daniel, Susan Solomon, On the climate forcing of carbon monoxide, J. Geophys. Res.: Atmos. 103 (D11) (1998) 13249–13260.
[58] SenterNovem, The Netherlands: list of fuels and standard CO 2 emission factors, Technical report, SenterNovem, 2005, URL www.broeikasgassen.nl.
[59] R Davis, L Tao, E C D Tan, M J Biddy, G T Beckham, C Scarlata, J Jacobson, K Cafferty, J Ross, J Lukas, D Knorr, P Schoen, Process Design and Economics for the Conversion of Lignocellulosic Biomass to Hydrocarbons: Dilute-Acid and Enzymatic Deconstruction of Biomass to Sugars and Biological Conversion of Sugars to Hydrocarbons, Technical report, 2013, www.nrel.gov/publications.
[60] Alison Mohr, Sujatha Raman, Lessons from first generation biofuels and implications for the sustainability appraisal of second generation biofuels, Effic. Sustain. Biofuel Prod.: Environ. Land-Use Res. 63 (2015) 281–310.
[61] FAO, Water for Sustainable Food and Agriculture Water for Sustainable Food and Agriculture, A Report Produced for the G20 Presidency of Germany, 2020, pp. 1–33, URL http://www.fao.org/3/i7959e/i7959e.pdf.
[62] Mette Hedegaard Thomsen, Anders Thygesen, Henning Jørgensen, Jan Larsen, Brge Holm Christensen, Anne Belinda Thomsen, Preliminary results on optimization of pilot scale pretreatment of wheat straw used in coproduction of bioethanol and electricity, in: Twenty-Seventh Symposium on Biotechnology for Fuels and Chemicals, Humana Press, 2007, pp. 448–460.
[63] Karen A. Beauchemin, H. Henry Janzen, Shannan M. Little, Tim A. McAllister, Sean M. McGinn, Life cycle assessment of greenhouse gas emissions from beef production in western Canada: A case study, Agric. Syst. 103 (6) (2010) 371–379.